Adsorbing surface strongly influences the pseudoperoxidase and nitrite reductase activity of electrode-bound yeast cytochrome *c*. The effect of hydrophobic immobilization

Lidia Lancellotti [a], Marco Borsari [a], Alois Bonifacio [c], Carlo Augusto Bortolotti [b], Giulia Di Rocco [b], Stefano Casalini [d], Antonio Ranieri [b,*], Gianantonio Battistuzzi [a,*], Marco Sola [b]

[a] *Department of Chemistry and Geology, University of Modena and Reggio Emilia, via Campi 103, 41125 Modena, Italy*
[b] *Department of Life Sciences, University of Modena and Reggio Emilia, via Campi 103, 41125 Modena, Italy*
[c] *Raman Spectroscopy Laboratory, Department of Engineering and Architecture, University of Trieste, Via Valerio 6a, Trieste, TS 34127, Italy*
[d] *Department of Chemical Sciences, University of Padova, via Marzolo 1, 35131 Padova, Italy*

ARTICLE INFO

Accepted 31 July 2020

Keywords:
Cytochrome *c*
Cardiolipin
Surface immobilization
Pseudoperoxidase
Nitrite reductase

ABSTRACT

The Met80Ala and Met80Ala/Tyr67Ala variants of *S. cerevisiae iso*-1 cytochrome *c* (ycc) and their adducts with cardiolipin immobilized onto a gold electrode coated with a hydrophobic self-assembled monolayer (SAM) of decane-1-thiol were studied through cyclic voltammetry and surface-enhanced resonance Raman spectroscopy (SERRS). The electroactive species - containing a six-coordinate His/His axially ligated heme and a five-coordinate His/- heme stable in the oxidized and reduced state, respectively - and the pseudoperoxidase activity match those found previously for the wt species and are only slightly affected by CL binding. Most importantly, the reduced His/- ligated form of these variants is able to catalytically reduce the nitrite ion, while electrode-immobilized wt ycc and other His/Met heme ligated variants under a variety of conditions are not. Besides the pseudoperoxidase and nitrite reductase functions, which are the most physiologically relevant abilities of these constructs, also axial heme ligation and the equilibria between conformers are strongly affected by the nature - hydrophobic vs. electrostatic - of the non-covalent interactions determining protein immobilization. Also affected are the catalytic activity changes induced by a given mutation as well as those due to partial unfolding due to CL binding. It follows that under the same solution conditions the structural and functional properties of immobilized ycc are surface-specific and therefore cannot be transferred from an immobilized system to another involving different interfacial protein-SAM interactions.

1. Introduction

Surface immobilization can impart cytochrome *c* (cytc) with diverse functional abilities *in vivo* and *in vitro* besides that of shuttling electrons which was thought to be the only role until about 15 years ago [1-11]. Key to this belief was the presence of the six-coordinate heme center featuring an His/Met axial ligation that would render the iron unavailable for substrate binding and thereby unable to carry out any catalytic action. Yet, cytc is involved in the regulation of oxidative stress, eliminating of H_2O_2 due to its peroxidase-like activity [12-14]. It has been eventually demonstrated that the "sixth" axial Met ligation is subjected to lifting or swapping following cytc peroxidation [12] and adsorption onto a structured molecular assembly. This happens under physiological conditions, as the binding to cardiolipin (CL), a negatively charged phospholipid of the inner mitochondrial membrane (IMM), that eventually leads to the apoptosis cascade [1-4,6,9,14-22], and upon tyrosine nitration and Met80 oxidation that induce cytc translocation from the mitochondrion to the cytoplasm and nucleus in non-apoptotic cells [14,23–28]. (Met)S-Fe bond breaking occurs also for cytc subjected to a non-covalent immobilization on surface-functionalized electrodes [29-34]. In both cases, cytc binding to the surface and the consequent motional restriction leads to the onset of a significant peroxidase and nitrite reductase activity that has important consequences for the programmed cell death and for applications in sensing interfaces and devices, respectively [6,9,17,18,30,33–37]. A great amount of work has been done on the physico-chemical behavior - including structural aspects,

* Corresponding authors.
E-mail addresses: antonio.ranieri@unimore.it (A. Ranieri), gianantonio.battistuzzi@unimore.it (G. Battistuzzi).

reactivity and catalysis - of cytochromes *c* from various sources immobilized on different surfaces under a variety of conditions [11,17,18,30–34,38–43].

Here, we focus on the role of the nature of the non-covalent interactions determining protein immobilization on the pseudoperoxidase and nitrite reductase functions, which are the most physiologically relevant abilities. It is conceivable that the adsorbing surface is not innocent, as the interfacial interactions may induce different effects on cytc conformation and orientation toward the solution which impact reactivity. To clarify this point it is important to measure such effects for given systems under controlled conditions and try to make considerations of general validity. To do so, in this work we focused on the Met80Ala and Met80Ala/Tyr67Ala variants of yeast *iso*-1 cytochrome *c* (ycc) which possess pseudoperoxidase and nitrite reductase activity when electrostatically immobilized on a negatively charged SAM-coated electrode [34,38,42,43] and studied if and how the structure of the heme center and the catalytic behavior change upon adsorption onto an hydrophobic SAM under the same conditions. We find that remarkable changes do occur indeed. It follows that the behavior of immobilized cytc is strongly affected by the properties of the adsorbing surface and that results cannot be transferred from an immobilized system to another. In addition, we found that the both mutations have a significant impact on the interaction of CL with ycc in the immobilized state.

2. Materials and methods

2.1. Materials

The Met80Ala and Met80Ala/Tyr67Ala mutants of recombinant *S. cerevisiae iso*-1 cytochrome *c* (M80A and M80A/Y67A hereafter) were expressed and isolated as described previously [34,38,39,42-44]. The variants are nontrimethylated and carry the C102T mutation to prevent protein dimerization [34,38,39,42-44]. Protein solutions were made up in 5 mM Tris-HCl and NaCl at pH 7.5 for storage at −20 °C. Solid decane-1-thiol (DT) and bovine cardiolipin (CL) in ethanolic solution were purchased from Sigma-Aldrich (catalog number 705233-1G and C1649, respectively). All chemicals were reagent grade. Doubly distilled water was used throughout.

2.2. Electrochemical measurements

A potentiostat/galvanostat mod. 273A (EG&G PAR, Oak Ridge, USA) was used to perform cyclic voltammetry (CV). Experiments were carried out using a cell for small volume samples (0.5 mL) under argon. A 1 mm-diameter polycrystalline gold wire, a Pt sheet, and a saturated calomel electrode (SCE) were used as working, counter, and reference electrode, respectively. The electrical contact between the SCE and the working solution was achieved with a Vycor® (from PAR) set. Reduction potentials were calibrated against the MV^{2+}/MV^{+} (MV = methyl viologen) and ferrocene/ferrocenium couples under all experimental conditions employed in this work to make sure that the effects of liquid junction potentials were negligible. All the reduction potentials reported here are referred to the standard hydrogen electrode (SHE), unless otherwise specified. The working gold electrode was cleaned as reported elsewhere [45]. The Vycor® set was treated in an ultrasonic pool for about 5 min. SAM coating on the gold electrode was obtained by dipping the polished electrode into a 1 mM ethanol solution of DT for 12 h and then rinsing it with water [17,46]. The functionalized electrode was then subjected to five voltammetric scans from + 0.2 to −0.3 V, 0 to −0.4 V, 0 to −0.6 V in 5 mM HEPES buffer, pH 7.2, to achieve SAM alignment [46]. Protein solutions were freshly prepared before use in 10 mM HEPES buffer at pH 7.2 and their concentration (typically 10 μM) was carefully checked spectrophotometrically (Jasco mod. V-570 spectrophotometer). Protein adsorption on the DT SAM-coated Au electrode was achieved by dipping the functionalized electrode into a 10 μM protein solution at 4 °C for 1 h. ycc–CL adducts were obtained by mixing cytochrome *c* and CL to obtain a 10 μM protein and 300 μM CL solution (ycc/CL molar ratio 1:30) in 10 mM HEPES at pH 7.2, which was allowed to stand for 30 min [17]. In these conditions, ycc is fully bound to CL as confirmed by the fluorescence spectra [17,18,47,48]. Adduct adsorption on the DT-coated electrode was achieved by dipping the functionalized electrode into the above solution for 1 h at 4 °C. The CV measurements were carried out using a working solution containing 10 mM sodium perchlorate and 10 mM HEPES buffer at pH 7.2. The electrochemical measurements were carried out avoiding the use of phosphate buffer. Indeed, phosphate ions at pH 7 are known to bind specifically to cytochrome *c* at the clustered surface lysines, thereby altering the interaction with CL and the properties of the resulting adduct [7,15,16,20,49–55]. 10 mM $NaClO_4$ was chosen as support electrolyte, since perchlorate features a single low-affinity interaction site on the surface of mitochondrial cyt, which is different from those proposed for phosphate [51] and the concentration used herein is much lower than that needed for specific binding [56].

From 5 to 35 °C, the voltammetric signals are reproducible and persist for several cycles, indicating a stable protein layer. The formal potentials E°' were calculated from the average of the anodic and cathodic peak potentials. CV measurements were performed at different scan rates v (from 0.02 to 40 V s^{-1}) and all the experiments were repeated at least five times. The reduction potentials were found reproducible within ± 0.001 V. Currents increase linearly with increasing the scan rate (not shown) and their ratio is almost unit throughout the temperature range studied, as expected for an adsorbed protein [57]. Surface coverage Γ_0 values for all species and their CL adducts were determined as reported previously [33,38]. Variable-temperature CV experiments were carried out with a cell in a "non-isothermal" setting, namely in which the reference electrode was kept at constant temperature (21 ± 0.1 °C) whereas the half-cell containing the working electrode and the Vycor® junction to the reference electrode was under thermostatic control with a water bath [58-63]. The temperature was varied from 5 to 30 °C. With this experimental configuration, the standard entropy change for heme Fe(III) to Fe(II) reduction in ycc ($\Delta S^{\circ\prime}_{rc}$) is given by [58–60]:

$$\Delta S^{\circ\prime}_{rc} = S^{\circ\prime}_{red} - S^{\circ\prime}_{ox} = nF\left(\frac{dE^{\circ\prime}}{dT}\right) \quad (1)$$

Thus, $\Delta S^{\circ\prime}_{rc}$ was determined from the slope of the plot of E°' versus temperature which turns out to be linear under the assumption that $\Delta S^{\circ\prime}_{rc}$ is constant over the limited temperature range investigated. With the same assumption, the enthalpy change ($\Delta H^{\circ\prime}_{rc}$) was obtained from the Gibbs-Helmholtz equation, namely as the negative slope of the E°'/T versus 1/T plot [61-64]. Repeated cycling does not affect the voltammograms from 5 to 30 °C, indicating that the protein monolayer is stable. The nonisothermal behavior of the cell was carefully checked by determining the $\Delta H^{\circ\prime}_{rc}$ and $\Delta S^{\circ\prime}_{rc}$ values of the ferricyanide/ferrocyanide couple [60–63].

Cyclic voltammograms at variable scan rate were recorded to determine the rate constant k_s for the interfacial electrochemical ET process for the adsorbed protein, according to Laviron [65]. Effects of uncompensated cell resistance were minimized using the positive-feedback *iR* compensation function of the potentiostat, set at a value slightly below that at which current oscillations emerge [66]. The k_s values were averaged over five measurements and found to be reproducible within 6%, which was taken as the

associate error. k_s values were also measured between 5 and 30 °C to determine the activation enthalpies ($\Delta H^{\#}$) using the Arrhenius equation, namely from the slope of the plot of ln k_s versus 1/T [17,29,32–34,38,40,43,45,46,49]. The electrocatalytic reduction of hydrogen peroxide and nitrite by immobilized ycc was studied by gradually adding aliquots of H_2O_2 and sodium nitrite solutions to the O_2-free cell solution at 5 °C [30,33,34,38,42]. The catalytic currents were measured as the difference between the cathodic peak current in the presence and in the absence of a given substrate concentration [30,42]. The catalytic current density (j) was calculated as the ratio of the electrocatalytic current i and the electrochemically determined area of the electrode. The area of the immersed portion of the gold wire was carefully calculated after each CV session by dipping the bare electrode at exactly the same depth into a solution of an electrochemical standard, ferrocenium tetrafluoborate, recording the CV signal for the standard, and then applying the Randles-Sevcik relationship [30,42].

2.3. Surface-enhanced resonance Raman spectroscopy

SERRS measurements on the electrode-immobilized cytochromes and their CL adducts were performed using a linearly moving spectroelectrochemical cell equipped with a flow system described elsewhere [32,34]. This configuration allows filling the cell with N_2-saturated buffer to minimize the presence of O_2 in contact with the working electrode. The working electrode was a 2.5-mm-diameter homemade nanostructured Ag electrode equipped with a removable Ag tip (SMARTIP Electrode, Mechanical Workshop of the Vrije University, Amsterdam). The counter and the reference electrode were a Pt plate embedded inside the polymeric body of the spectroelectrochemical cell and a SCE (AMEL Instruments, Milan), respectively. Ag electrodes were polished and roughened as described previously [67,68]. Spectra were collected in back-scattering geometry, with an InVia Raman microscope (Renishaw plc, Wotton-under-Edge, U.K.) equipped with a Bluephoton 405 nm diode laser (Omicron GmbH, Rodgau-Dudenhofen, Germany) delivering 0.5 mW laser power at the sample and with a spectrograph having a 2400 l/mm grating (spectral resolution of approximately 4 cm^{-1}) and a thermoelectrically cooled (-70 °C) CCD camera [32,34]. Spectra were collected with an exposure time of 30 s. The spectrograph was calibrated using the lines of a Ne lamp. A 60 × water immersion microscope objective (NA = 1.00) was used to focus the laser on the surface of the DT-coated roughened Ag electrodes on which the protein had been adsorbed [32,34]. SAM formation was achieved exposing the roughened electrode to a 1-mM ethanol solution of DT for 12 h. The procedure for immobilizing ycc and their CL adducts on the DT-coated Ag working electrode was identical to that used for the CV measurements. The reference electrode and the cell were kept at constant room temperature (20 °C). During each measurement, the electrode was kept moving using a motorized microscope stage (Prior Scientific Instruments Ltd., Cambridge, UK) to renew the part of the electrode surface illuminated by the laser, thus avoiding overheating and/or sample photodegradation. SERRS measurements were performed in three independent replicas (i.e. on three different electrodes). To facilitate comparison, all spectra were baseline-subtracted (polynomial baseline) and vector-normalized.

3. Results and discussion

3.1. Voltammetry and oxidation state-dependent heme coordination

The two variants and their CL-adducts show the same voltammetric behavior that matches that of wt ycc and its triple KtoA variant studied previously under the same conditions [17,18]. These mutations do not alter the redox state-dependent heme iron axial coordination found for wt, as shown by the SERRS data discussed below. In particular, two redox-state-dependent electroactive conformers are observed, indicated as LP and HP, which are most stable in the oxidized and reduced state, respectively. LP corresponds to a low-spin (LS) six-coordinate (6c) His/His-ligated heme containing species in which the OH^- ion, which substitutes the native Met80 as heme axial ligand in both mutants [34,38,42–44,69–71], is replaced by a His residue (either His26 or His33) [1,3,7,15–18,24,53,72–74], while HP contains a high-spin (HS) five-coordinate (5c) His/- ligated heme, in which iron features an open coordination site due to the detachment of the axial OH^- ligand [17,18]. As for wt, the reduced 6c LP and the oxidized 5c HP conformers convert with time into the stable reduced 5c HP and oxidized 6c LP species, respectively [17]. Indeed, at scan rates (υ) lower than 0.1 Vs^{-1}, the voltammograms - run in either cathodic or anodic direction - contain the peaks LP_c(intense)/LP_a(weak) and HP_c(weak)/HP_a(intense) (Fig. 1). Upon increasing υ, these transitions have no time to occur, therefore in the anodic (cathodic) scan the current of LP_a (HP_c) increase (Fig. 2). At υ above 5 V s^{-1} the two redox couples are clearly visible (Fig. 2) and their E°' values can be determined safely (Table 1).

Mutations have an impact on the thermodynamic and kinetic parameters of the redox reaction and species conversion. The E°' values for the variants and their adducts with CL are quite similar, as found for wt and its triple KtoA mutant [17,18]. The ratio of the peak areas Q_{LPc}/Q_{HPc} (where Q_{LPc} and Q_{HPc} are the charge needed to reduce the oxidized adsorbed 6c LP and 5c HP protein, respectively) is independent of scan rate, indicating that the surface concentration of the two forms is constant. While this ratio does not change appreciably with temperature for wt, it does for M80A and M80A/Y67A (Fig. 3). Also the Q_{LPa}/Q_{HPa} ratio is independent of scan rate and is strongly affected by temperature. In particular, peak LP_a decreases with increasing temperature while peak HP_a increases (Fig. 3). Thus, interconversion between the ferrous high-spin 5c His/- (HP) and low-spin 6c His/His (LP) species is affected by temperature. The Q_{LPa}/Q_{HPa} ratio can be taken as the ratio between the corresponding protein surface concentration ($\Gamma_{LPa}/\Gamma_{HPa}$). Under the hypothesis that the activity of the adsorbed species is equal to the corresponding surface concentration ($a_{LPa} = \Gamma_{LPa}$, and $a_{HPa} = \Gamma_{HPa}$), such current ratio yields the equilibrium constant, $K_{HP\rightarrow LP}$, for the above transition at each temperature (Table 2). The standard enthalpy and entropy changes, $\Delta H^{\circ}_{HP\rightarrow LP}$ and $\Delta S^{\circ}_{HP\rightarrow LP}$, associated to the HP to LP transition can be calculated from the vant'Hoff equation (Fig. 4, Table 2) [17]. The same constant for the oxidized species and the corresponding thermodynamic parameters could not be measured as above because the cathodic signal of the HP form is weak and not well resolved. Therefore, a Born-Haber cycle was used, taking advantage of the ΔH°_{rc} and ΔS°_{rc} values for the LP and HP species discussed below (Scheme 1, Supplementary Information). As expected, the $K_{HP\rightarrow LP}$ values for the oxidized forms are remarkably higher than the reduced forms, due to the much larger affinity of the ferric ion for the bis-His axial ligation of the 6c LP state. Bonding interactions (enthalpic term) invariably favor the transition, particularly for the ferric state, consistent with the formation of an additional coordination bond in LP. This effect is opposed by relevant entropic costs, much less oxidation state-dependent, likely contributed by a decrease in the motional degrees of freedom of the protein, consistent with some structuring effects due to the additional linkage, but largely due to transition induced changes in the solvation properties of the heme and the protein as a whole.

For all species in both redox states, formation of the CL adducts decreases the $K_{HP\rightarrow LP}$ values. In the two mutants the observed effect has an enthalpic origin, whereas for wt the effect is entirely entropic in nature. Conceivably, CL stabilizes the 5c His/- form and

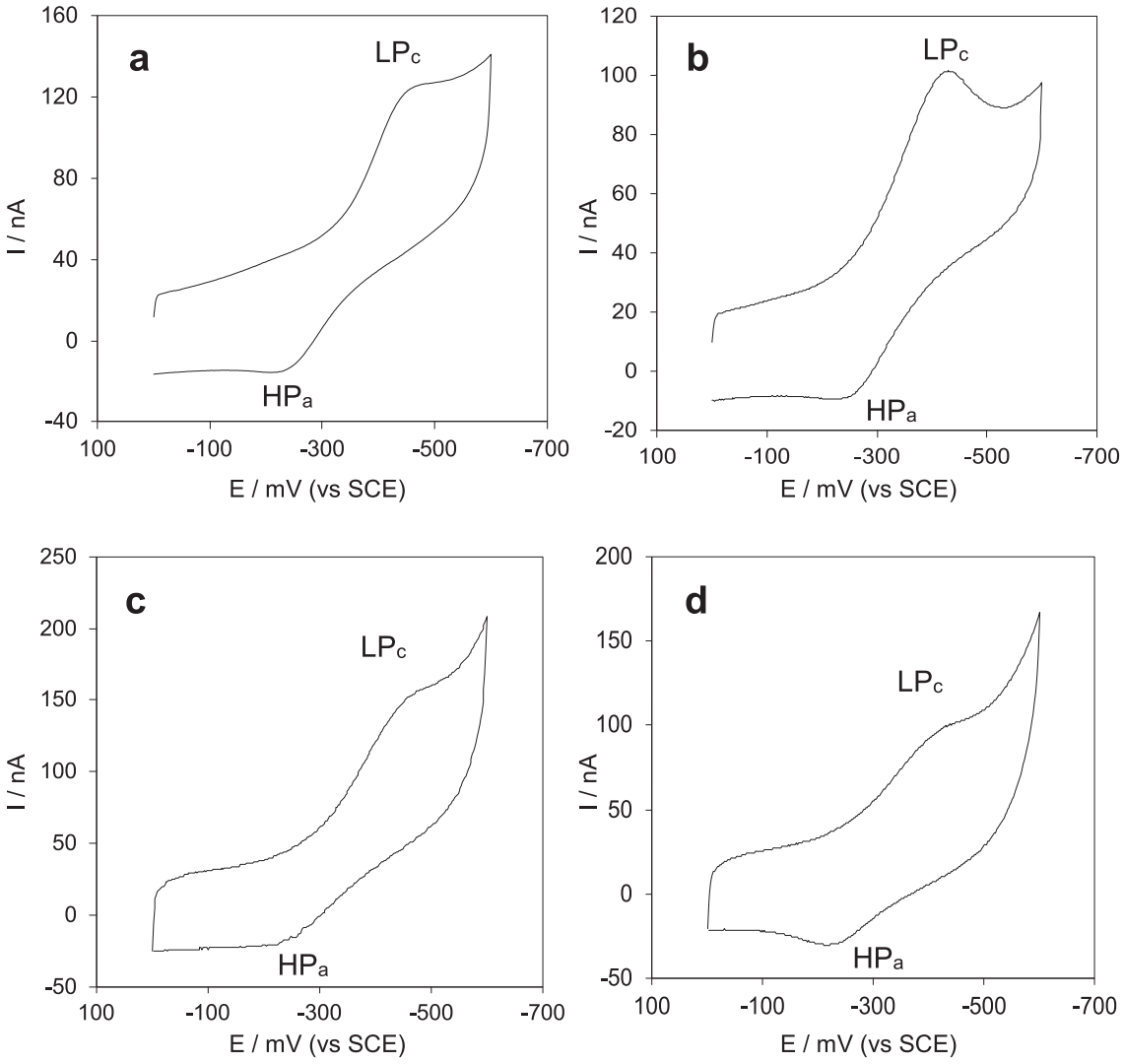

Fig. 1. Cyclic voltammograms at low scan rate (0.05 V s^{-1}) for (a) the M80A and (b) the M80A/Y67A variant of *Saccharomyces cerevisiae* yeast *iso*-1 cytochrome *c* immobilized on a hydrophobic SAM of decane-1-thiol (DT) and (c) and (d) the corresponding adducts with cardiolipin immobilized under the same conditions. Potentials are vs. SCE. Potential scans started from E = +0.0 V. Working solution: 10 mM sodium perchlorate and 10 mM HEPES buffer at pH 7.2. T = 278 K.

obstacles formation of the additional bond, possibly by introducing some structural constraints to iron coordination of the second axial His. Overall, mutations significantly affect the interaction of CL with ycc on the DT SAM. We note that for the proteins and their CL-adducts in both redox states $K_{HP\rightarrow LP}$ increases in the order: wt, M80A, M80A/Y67A. The change due to the M80A mutation is dominated by a decrease in the entropic cost of the transition most likely due to solvation effects related to the mutation-induced increased exposure of the heme center to solvent, while increasingly relevant enthalpic effects are generated by the additional Y67A mutation (Table 2). The importance of transition-induced reorganization of the H-bonding network at protein-solution interfaces on the thermodynamics of the process is demonstrated by the characteristic [17,29,34,49,75-90] enthalpy/entropy compensation shown by the $\Delta H^{\circ}_{HP\rightarrow LP}$ and $S^{\circ}_{HP\rightarrow LP}$ values of each protein (Fig. S1).

3.2. SERR spectroscopy: Axial heme iron ligation

Surface-enhanced resonance Raman (SERR) spectroscopy yields structural insight into the coordination features of the heme center of cytochromes *c* [91] as certain heme vibrational modes are distinctive of the iron oxidation state, spin state and coordination number [92,93]. In particular, the ν_2, ν_3, ν_4 and ν_{10} bands, according to Abe et al. are usually taken as marker bands [94]. The Raman shifts and band intensities in the RR spectrum of oxidized M80A in solution at pH 7 (Fig. S2) are indicative of a low-spin six-coordinate heme iron axially bound to the proximal His residue and a hydroxide ion (His-Fe-OH) [44]. For the M80A protein, however, a band at 1570 cm^{-1} is suggesting that a fraction of the protein might be unfolded to yield a high-spin six-coordinate heme iron containing form, possibly with a H_2O/H_2O axial ligation [74]. The same species immobilized on an anionic SAM of 11-mercapto-1-undecanoic acid (MUA) and 11-mercapto-1-undecanol (MU) (MUA/MU hereafter) feature the 6c LS heme with a His/OH^- axial coordination observed in solution, which is almost unaffected upon 7 M urea-induced unfolding [34]. On the contrary, spectral changes are found in the SERR spectra for both oxidized M80A and M80A/Y67A adsorbed on the DT-coated electrode (Fig. 5). In particular, besides the invariant band ν_4 at 1374 cm^{-1} (consistent with a 6c LS state), the spectra display a shift in the ν_3 bands at 1504 and 1506 cm^{-1} for the M80A and M80/Y67A, respectively. While still characteristic of a 6cLS species, such values suggest a change in one of the heme axial ligand, possibly a His/His or a His/H_2O coordination [74]. The

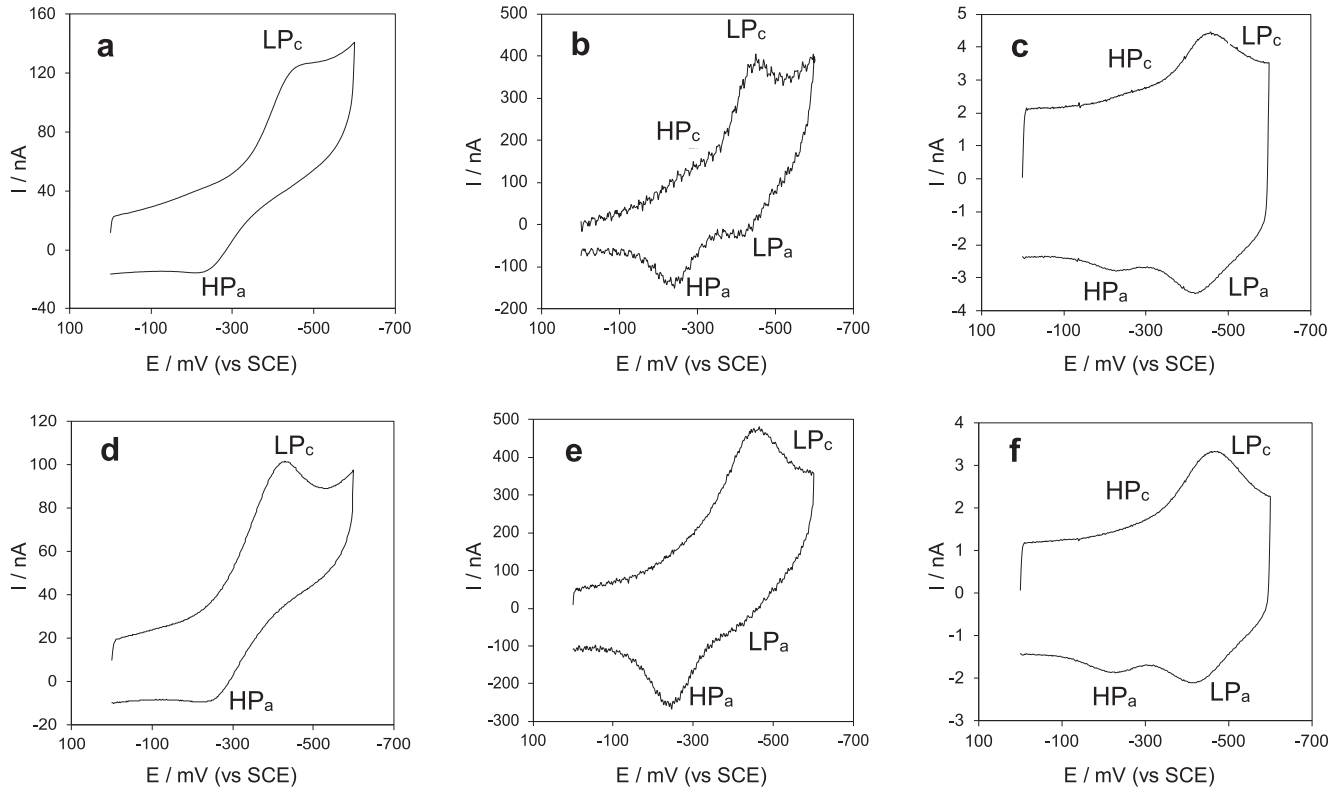

Fig. 2. Cyclic voltammograms at variable scan rate for (a–c) the M80A and (d–f) the M80A/Y67A variant the recombinant *Saccharomyces cerevisiae* yeast *iso*-1 cytochrome *c* immobilized on a hydrophobic SAM of decane-1-thiol (DT); Scans were started after an oxidizing poise at E = +0.0 V followed by an anodic scan. Potentials are vs. SCE. Scan rate: (a, d) 0.05 Vs^{-1}; (b, e) 1 Vs^{-1}; (c, f) 5 Vs^{-1} Very similar responses were obtained from the corresponding adducts with cardiolipin immobilized under the same conditions. Working solution: 10 mM sodium perchlorate and 10 mM HEPES buffer at pH 7.2. T = 278 K.

Table 1
Thermodynamics of reduction and kinetics of heterogeneous electron transfer for wild-type *Saccharomyces cerevisiae* yeast *iso*-1-cytochrome *c* (ycc), its M80A and M80A/Y67A variants and their cardiolipin adducts (+CL) adsorbed on a gold electrode coated with decane-1-thiol.[a]

		$E^{\circ\prime}$ (V)[c]		$\Delta H^{\circ\prime}_{rc}$ (kJ mol^{-1})[d]		$\Delta S^{\circ\prime}_{rc}$ (J mol^{-1} K^{-1})[e]		k_s (s^{-1})[f]		$\Delta H^{\#}$ (kJ mol^{-1})[g]		ln*A*	
		free	+CL	free	+CL	free	+CL	free	+CL	free	+CL	free	+CL
M80A	LP	−0.182	−0.172	46.2	42.2	95	87	349	69	10.6	12.5	10.2	9.4
	HP	0	0	12.3	14.9	43	51	201	44	12.7	13.8	10.5	9.5
M80A/Y67A	LP	−0.190	−0.194	55.1	48.5	125	102	189	70	12.4	15.1	10.3	10.5
	HP	0	−0.006	17.1	23.2	59	77	107	69	14.7	17.1	10.7	11.3
wt [b]	LP	−0.253	−0.226	55.4	48.3	106	90	339	232	7.9	8.3	9.1	8.9
	HP	−0.106	−0.101	27.2	23.9	57	48	127	119	9.8	10.1	8.9	8.9
KtoA[b]	LP	−0.270	−0.248	46.2	48.8	69	85	186	131	8.5	8.8	8.9	8.7
	HP	−0.111	−0.106	27.7	26.1	58	54	97	85	9.1	9.5	8.5	8.6

[a] LP and HP correspond to the 6c His/His-ligated and the 5c His/- ligated heme-containing form, respectively. The average error on $E^{\circ\prime}$, $\Delta S^{\circ\prime}_{rc}$, $\Delta H^{\circ\prime}_{rc}$, *ks*, $\Delta H^{\#}$ and ln*A* are ± 0.001 V, ±2 J K^{-1} mol^{-1}, ±0.8 kJ mol^{-1}, ±6%, ±0.2 kJ mol^{-1} and ± 0.2, respectively. Working solution: 10 mM sodium perchlorate and 10 mM HEPES buffer at pH 7.2.
[b] From ref. [17,18].
[c] T = 278 K.
[d] $\Delta H^{\circ\prime}_{rc}$: standard enthalpy change for Fe(III) to Fe(II) ycc reduction.
[e] $\Delta S^{\circ\prime}_{rc}$: standard entropy change for Fe(III) to Fe(II) ycc reduction;
[f] k_s: rate constant for the heterogeneous electrode-ycc electron transfer. T = 278 K.
[g] $\Delta H^{\#}$: activation enthalpy for the heterogeneous electrode-ycc electron transfer.

ν_3 band of the M80A on DT, moreover, displays a shoulder at lower wavenumbers, compatible with the occurrence of a 5cHS species. In the presence of CL, however, the spectrum of M80A remains almost unchanged (if not by a decrease of the 5cHS ν_3 shoulder), whereas that of M80A/Y67A shows a clear band at 1494 cm^{-1}, indicating the conversion of a fraction of the protein to a 5cHS species.

These results indicate that *a)* heme axial ligation in M80A and M80/Y67A immobilized on a hydrophobic surface, either free or bound to CL, differs from that of the same species in solution and electrostatically immobilized on MUA/MU and *b)* CL binding does not affect appreciably the coordination of the heme center for M80A (while it affects M80A/Y67A), in full agreement with the electrochemical data discussed above. Therefore, while immobilization on anionic SAM does not affect the heme iron binding set of the solution species, even in the presence of high concentrations of an unfolding agent such as urea, immobilization on a hydrophobic DT SAM does. Both DT-immobilized ferric ycc vari-

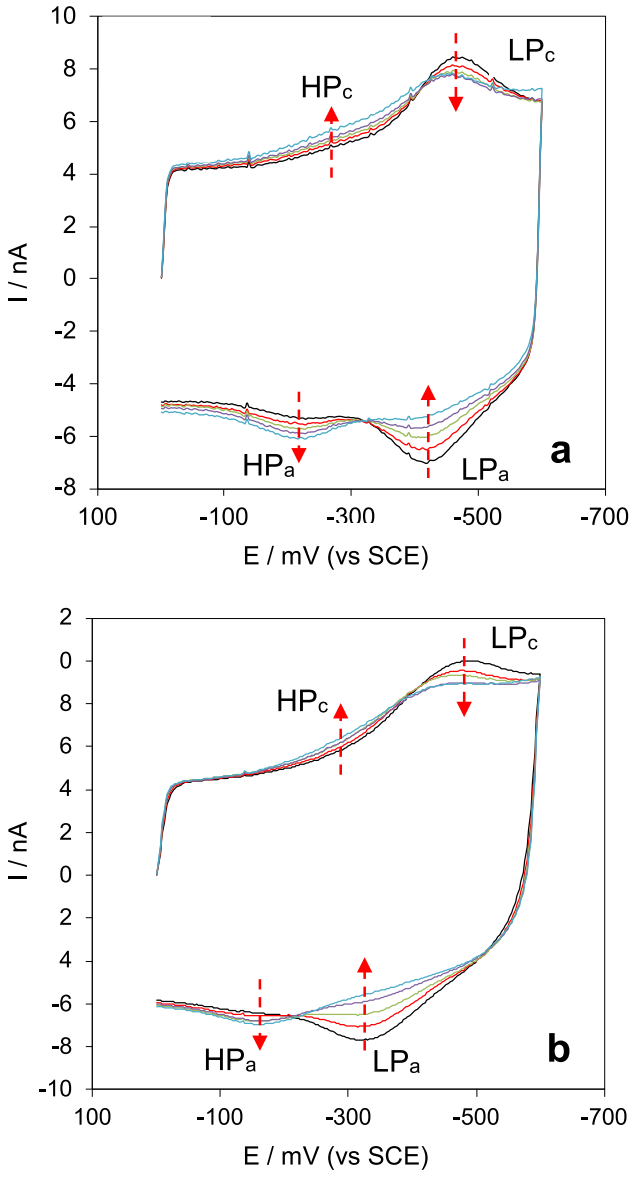

Fig. 3. Cyclic voltammograms at variable temperature for (a) the M80A and (b) the M80A/Y67A variant the recombinant *Saccharomyces cerevisiae* yeast *iso*-1 cytochrome *c* immobilized on a hydrophobic SAM of decane-1-thiol (DT). The arrows indicate the changes observed with increasing temperature from 278 to 298 K. Black: T = 278 K; red: T = 283 K; green: T = 288 K; magenta: T = 293 K; light blue: T = 298 K. Scans were started after an oxidizing poise at E = + 0.0 V followed by an anodic scan. Potentials are vs. SCE. Scan rate, 10 Vs^{-1}. The corresponding adducts with cardiolipin immobilized under the same conditions yielded very similar responses. Working solution: 10 mM sodium perchlorate and 10 mM HEPES buffer at pH 7.2.

ants and their CL adducts appear, as wt ycc, as a mixture of a prevailing form with a 6c LS His/His ligated heme and another less abundant form featuring a high-spin heme in which the sixth ligand is lacking. A His/His axial heme ligand set was found previously also for ferricytochrome *c* in a hydrophobic micellar environment [72,73]. His26 and His33 were suggested as candidates to serve as sixth ligand [16,53,72,95,96]. These residues are distant from the heme iron in the native structure, but their binding could be the result of protein unfolding due to the hydrophobic immobilization, eventually modulated by the presence of CL.

From the above, the LP and HP forms should contain a 6c His/His and a 5c His/- center, respectively. The presence of a His residue as the sixth axial heme iron ligand in the ycc-CL adducts – that experience a motional restriction as that due to the binding to IMM - would be consistent with the peroxidase activity of CL-bound cytc. In fact, the His/His ligated cytc shows both pseudo peroxidase [15-17,24,30,31,33,97,98] and nitrite-reductase activities [34,96] and catalyzes the reduction of dioxygen to superoxide anion [18,99]. All activities are functional to the peroxidation of CL by cytc at the onset of the apoptotic cascade [14,35,100]. Overall, these data provide compelling evidence that axial heme iron coordination in ycc, regardless of mutations in the heme crevice and CL binding, is responsive to the electrostatic or hydrophobic nature of the noncovalent protein-SAM interactions.

3.3. Redox thermodynamics of the adsorbed species

The E°' values for the HP and LP forms of both variants and their CL adducts increase linearly with increasing temperature (Figure S3). The reduction thermodynamics are listed in Table 1. The two variants show E°' values higher than wt by approximately 0.07 and 0.11 V for the LP and HP form, respectively. Hence, stabilization of the reduced heme is somewhat larger for the 5c His/- form, which is that poised for reductive catalysis. In general, the E°' increase upon CL complexation is small; the only significant effect being that for the LP form of wt (+0.027 V). For the CL adducts, mutation-induced stabilization of the ferrous HP form is the same as above, while it is lower for the LP form. As wt and the variants all feature a His/His axial heme coordination, stabilization of the reduced state due to mutations, which turns out to be mostly enthalpic in nature for M80A and entropic for the double variant, regardless of CL complexation, can be assigned to the increase in hydrophobicity of the heme environment, enhanced in the CL adducts by insertion of the CL hydrophobic chain inside the heme pocket. This would stabilize the ferrous heme that bears a lower charge (0 vs. + 1 of the ferric form). Concomitant solvent reorganization effects most likely occur, which are particularly relevant in the double variant due to the dominant entropic contributions to the E° changes.

3.4. Kinetics of protein-electrode electron transfer

The heterogeneous rate constants (k_s) for the electron transfer process for M80A and M80A/Y67A are listed in Table 1. As shown by Bowden et al., the k_s values obtained with the Laviron method can be assumed to correspond to the kinetic constant for ET at zero driving force [33,101-103]. Therefore, k_s can be written as [104]:

$$k_s = \upsilon_0 \cdot e^{[-\beta\cdot(r-r_0)]} \cdot e^{-\Delta G^{\#}/RT} \quad (2)$$

namely:

$$k_s = \upsilon_0 \cdot e^{[-\beta\cdot(r-r_0)]} \cdot e^{\Delta S^{\#}/R} \cdot e^{-\Delta H^{\#}/RT} \quad (3)$$

Hence, we can discuss the effects of point mutations and CL binding on k_s, $\Delta H^{\#}$ and the pre-exponential factor A ($=\upsilon_0 \cdot e^{[-\beta\cdot(r-r_0)]} \cdot e^{\Delta S^{\#}/R}$) (Table 1, Fig. S4). Previous studies on *wt* and mutated ycc immobilized of different SAMs [17,29,33,34,87] indicated that the activation enthalpy mainly depends on the polarizability and solvent accessibility of the heme crevice. The pre-exponential factor A is mainly controlled by protein-SAM interactions including surface-specific entropic contributions to the reorganization energy and/or changes in the tunneling factor β and in the distance r of the heterogeneous ET between the heme and the electrode [29,32,33,38,43,45,46,87].

The LP and HP conformers of both mutants feature larger $\Delta H^{\#}$ and A values compared to the corresponding forms of wt that partially offset resulting in rather limited changes in k_s (Table 1 and Fig. S5). The mutation-induced increase in the activation enthalpy

Table 2
Thermodynamic parameters for the HP → LP transition occurring for wild-type *Saccharomyces cerevisiae* yeast *iso*-1-cytochrome *c* (ycc), its M80A and M80A/Y67A variants and their cardiolipin adducts (+CL) adsorbed on a gold electrode coated with decane-1-thiol.[a]

			$K_{HP→LP\ (278\ K)}$	$\Delta H^{\circ}_{HP→LP}$ (kJ mol^{-1})	$\Delta S^{\circ}_{HP→LP}$ (J mol^{-1} K^{-1})
wt [b]	free	Fe(II)	0.30 ± 0.02	−53.1 ± 1.8	−204 ± 9
		Fe(III)	212 ± 18	−81.6 ± 2.8	−249 ± 10
	+CL	Fe(II)	0.13 ± 0.01	−56.8 ± 1.9	−221 ± 11
		Fe(III)	37 ± 3	−81.2 ± 2.9	−262 ± 12
M80A	free	Fe(II)	4.12 ± 0.18	−44.7 ± 1.6	−149 ± 8
		Fe(III)	4.94 ± 0.44x10^4	−78.9 ± 1.8	−194 ± 10
	+CL	Fe(II)	2.93 ± 0.12	−29.5 ± 1.4	−97 ± 6
		Fe(III)	1.25 ± 0.15x10^4	−57.1 ± 1.9	−127 ± 8
M80A/Y67A	free	Fe(II)	9.91 ± 0.43	−50.2 ± 1.7	−162 ± 9
		Fe(III)	1.64 ± 0.14x10^5	−88.9 ± 2.7	−220 ± 11
	+CL	Fe(II)	4.95 ± 0.29	−35.1 ± 1.6	−113 ± 12
		Fe(III)	7.00 ± 0.68x10^4	−60.8 ± 1.8	−126 ± 15

[a] Working solution: 10 mM sodium perchlorate and 10 mM HEPES buffer at pH 7.2.
[b] From ref. [17,18].

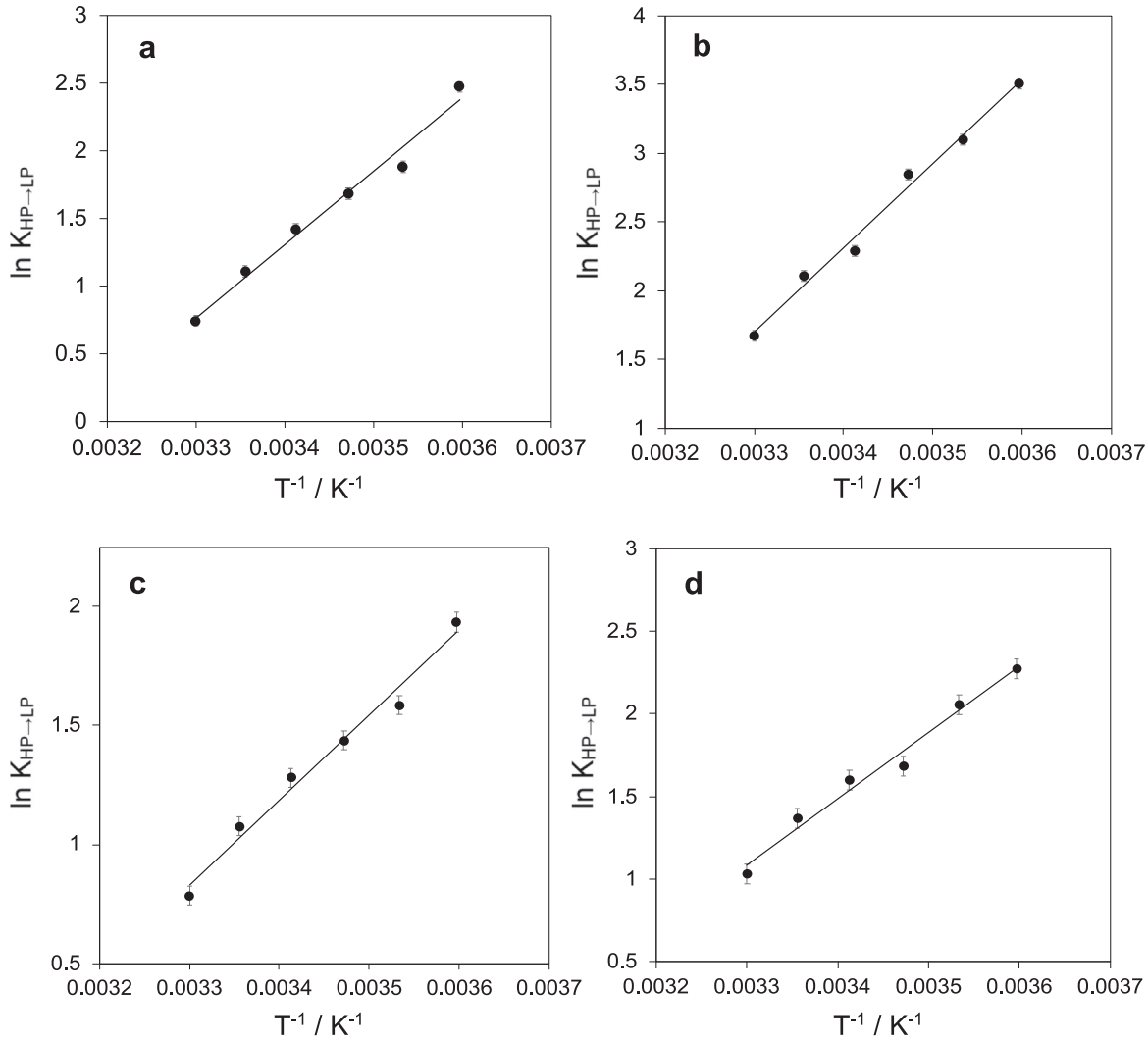

Fig. 4. van't Hoff plot for the equilibrium constant ($K_{HP→LP}$) for the high spin 5c His/- (HP) to low spin 6c His/His (LP) transition for a) the reduced M80A and b) the reduced M80A/Y67A variant of *Saccharomyces cerevisiae* yeast *iso*-1 cytochrome *c* immobilized on a hydrophobic SAM of decane-1-thiol (DT) and c) and d) the corresponding adducts with cardiolipin immobilized under the same conditions. Scan rate, 10 Vs^{-1}. Working solution: 10 mM sodium perchlorate and 10 mM HEPES buffer at pH 7.2.

is possibly due to an increase in reorganization energy due to a modified reduction-induced change in the number and structure of water molecules in the heme crevice. Such an increase is invariably larger for the double variant compared to M80A. Interestingly, the LP and HP conformers of both mutants show similar $\Delta\Delta H^{\#}$ (=$\Delta H^{\#}_{mutant}$ - $\Delta H^{\#}_{wt}$) values, hence the effects of the mutation-induced increases of activation enthalpy on the k_s of both conformers are comparable (Table 1). The larger values of the pre-exponential fac-

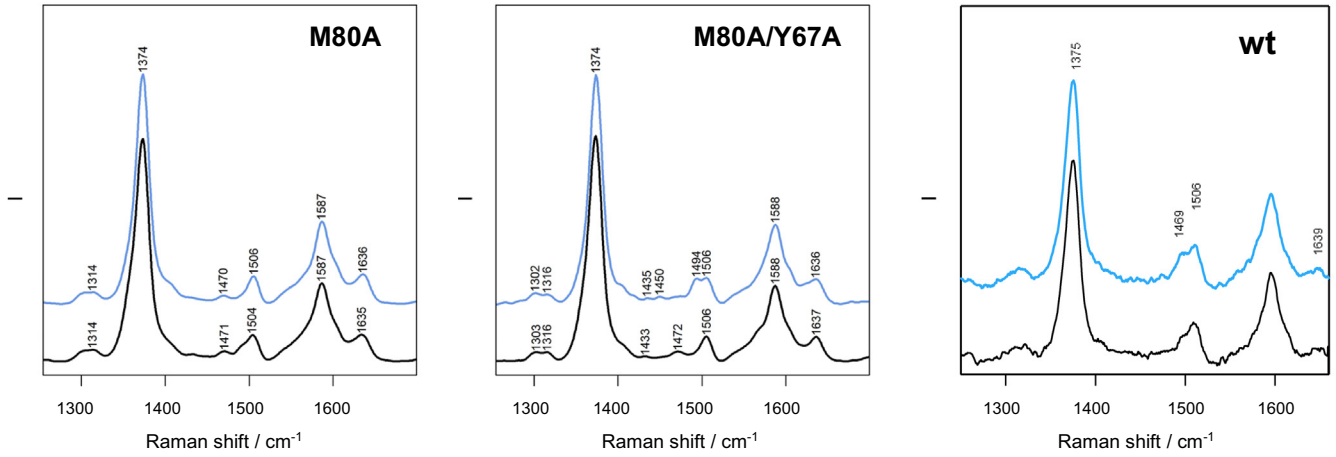

Fig. 5. SERRS spectra for the oxidized wt yeast *iso*-1-cytochrome *c* (from ref [18]) and its M80A and M80A/Y67A variants in the high-frequency region recorded with a 405 nm excitation line immobilized on a hydrophobic SAM of decane-1-thiol (DT): free protein (black trace); CL-adduct (blue trace). Measurements were performed in 10 mM sodium perchlorate and 10 mM HEPES buffer at pH 7.2. T = 293 K. Spectra were corrected by subtracting a linear baseline.

tor *A* for both mutants compared to wt suggest that the mutations sensibly alter protein-DT interactions, inducing a lowering of the tunneling factor and/or a different distribution of the water molecules at the SAM-protein interface which affects $\Delta S^{\#}$.

CL binding invariably slows down the heterogeneous electron transfer in a protein-dependent fashion, mostly due to an increase in the activation enthalpy (Table 1 and Fig. S5). The CL-induced enhancement of $\Delta H^{\#}$ is quite limited for both conformers of wt

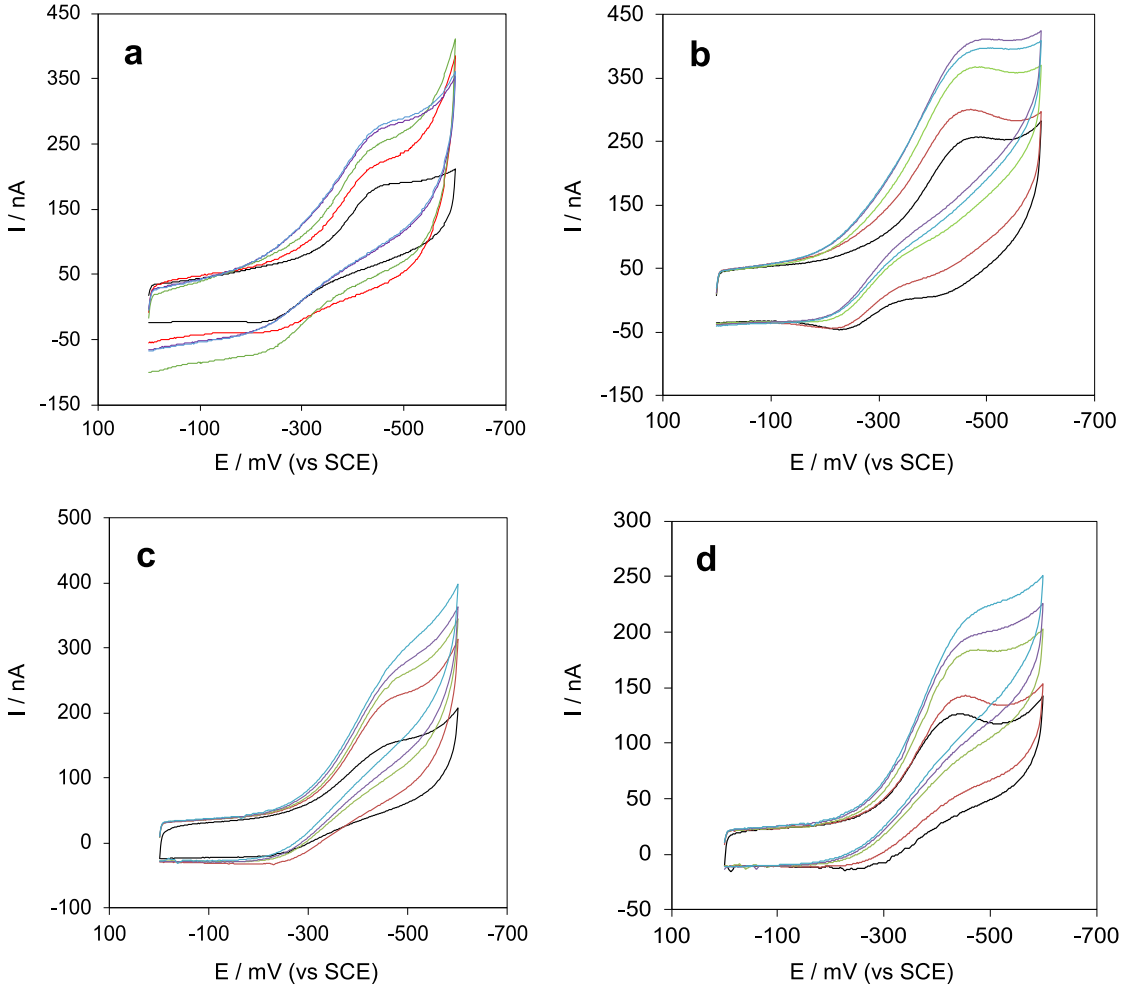

Fig. 6. Cyclic voltammograms for a) the M80A and b) the M80A/Y67A variant of *Saccharomyces cerevisiae* yeast *iso*-1 cytochrome *c* immobilized on a hydrophobic SAM of decane-1-thiol (DT) and c) and d) the corresponding adducts with cardiolipin immobilized under the same conditions. at increasing H_2O_2 concentration: 0 μM (black), 1 μM (red), 2 μM (light green), 3 μM (purple), 4 μM (light blue). Working solution: 10 mM sodium perchlorate and 10 mM HEPES buffer at pH 7.2. T = 278 K. Scan rate 0.05 V s^{-1}.

but is much more relevant for M80A and M80A/Y67A. Analogously, CL does not change the pre-exponential factor for wt but modifies it in both variants (Table 1 and Fig. S5). Hence, CL binding likely has an impact on both the reduction-induced changes in the hydration of the heme crevice of both mutants and their interaction with the DT SAM, while it barely affects wt ycc. This indicates that the changes in the accessibility and the H-bonding network in the heme crevice due to the M80A and M80A/Y67A mutations significantly modifies CL binding to ycc on the DT-SAM, in line with the data on the $K_{HP\rightarrow LP}$ values discussed above. These changes are only slightly affected by the coordination number of the heme iron, as the CL-induced effect observed for the LP and HP conformers of the same protein are very similar (Table 1 and Fig. S6).

We note that the k_s values for the proteins in the absence of CL (free protein hereafter) are sensibly higher than those for the same proteins immobilized of a MUA/MU SAM [17,29,34] as a result of larger ln*A* values (since the activation enthalpies are conserved). Therefore protein-SAM interactions have an impact on the tunneling factor and reorganization of water molecules at the SAM-protein interface that affect the preexponential factor. This also tells us that the nature of the SAM may affect the electrocatalytic properties of these adsorbed species (discussed below) that involve protein-electrode ET.

3.5. Pseudo peroxidase and nitrite-reductase activity

The cyclic voltammograms for the immobilized proteins, recorded in the presence of increasing micromolar concentrations of hydrogen peroxide and sodium nitrite at pH 7.2, are shown in Figs. 6 and 7, respectively. For both variants, the cathodic (anodic) currents increase (decrease) with increasing hydrogen peroxide and nitrite concentration, with a typical catalytic behavior indicating that the adsorbed proteins catalyze the reduction of H_2O_2 (pseudo peroxidase activity) and NO_2^- (nitrite-reductase activity). The current of the cathodic peak LP increases with almost no change in peak potential. This indicates that the catalytically active form of the proteins, i.e. the form which interacts with H_2O_2 and NO_2^-, is the reduced His/His-ligated form state, as previously found for wt ycc and its CL-adduct on DT versus H_2O_2 while the same variants subjected to urea unfolding on MUA/MU carry out catalysis using a His/OH^- axial heme iron coordination [17,30,33,34]. The currents of the cathodic peak HP are barely detectable and there-

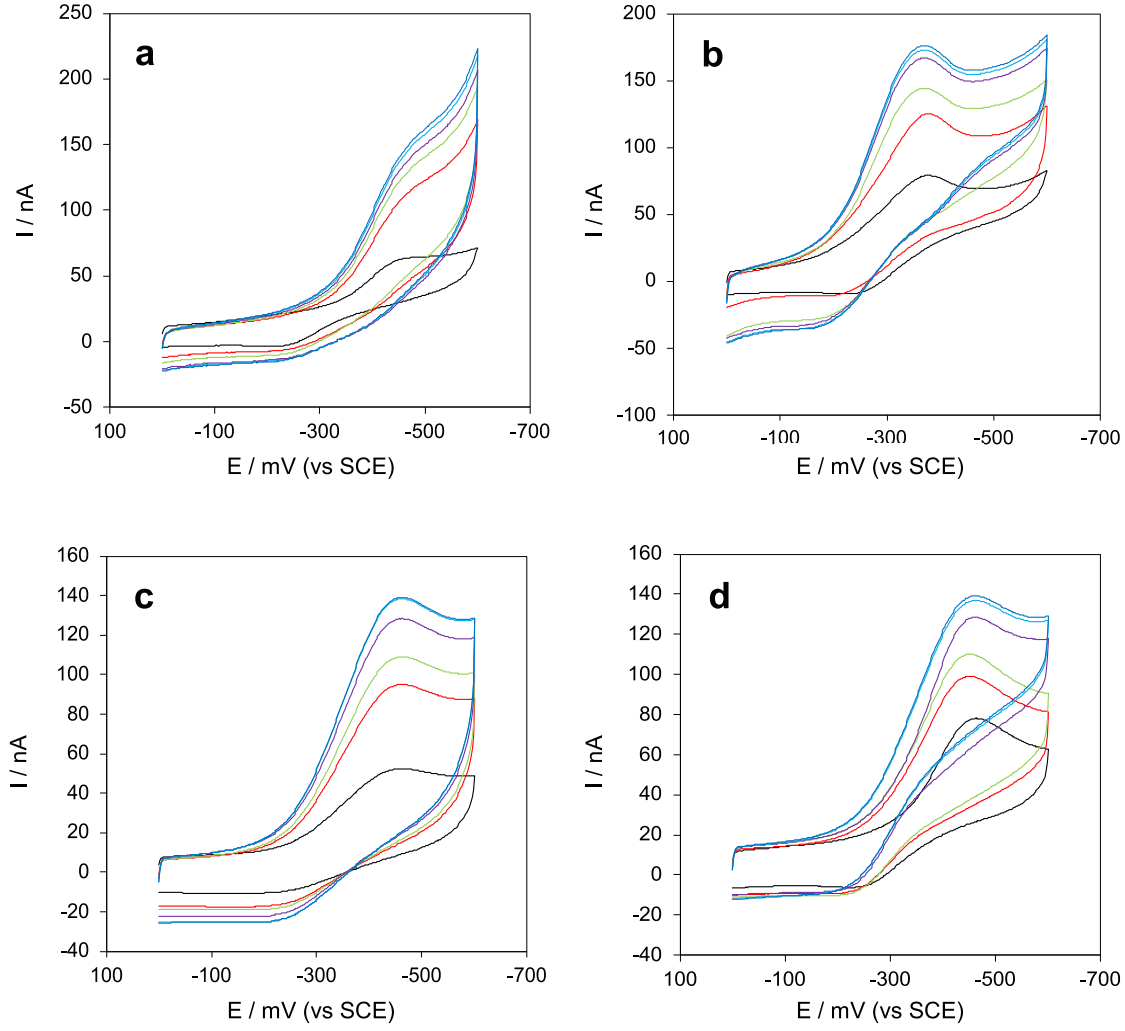

Fig. 7. Cyclic voltammograms for (a) the M80A and (b) the M80A/Y67A variant of *Saccharomyces cerevisiae* yeast *iso*-1 cytochrome *c* immobilized on a hydrophobic SAM of decane-1-thiol (DT) and c) and d) the corresponding adducts with cardiolipin immobilized under the same conditions at increasing sodium nitrite concentration: 0 μM (black), 0.25 μM (red), 0.5 μM (light green), 1 μM (purple), 1.5 μM (light blue), 1.75 μM (dark blue). Working solution: 10 mM sodium perchlorate and 10 mM HEPES buffer at pH 7.2. T = 278 K. Scan rate 0.05 V s^{-1}.

fore were not taken into account in the measurement of the electrocatalytic activity. Immobilized folded wt ycc is catalytically inactive because the six-coordinate heme iron is not available for substrate binding as Fe(II) binds strongly to the thioether sulfur of the Met ligand [30,33,38]. The electrocatalytic effect occurs up to H_2O_2 and NO_2^- concentrations of about 5 μM and 1.75 μM, respectively, above which the cathodic currents irreversibly decrease. Below these substrate concentrations limits, elimination of hydrogen peroxide or nitrite (obtained by rinsing the electrode with buffer) restored the CV signal of the protein. Catalytic currents could then be re-obtained upon hydrogen peroxide or sodium nitrite addition. Therefore, under these conditions the protein layer is stable and re-usable. No additional peaks were detected in the potential range from + 0.6 to −0.8 V (vs. SCE) at all hydrogen peroxide and sodium nitrite concentrations investigated.

The catalytic activity of electrode-immobilized proteins can be estimated from the Michaelis-Menten model expressed in terms of current density and reported as Lineweaver-Burk plots: [17,30,33,34,38,42,105,106]

$$\frac{1}{j_{cat}} = \frac{1}{j_{max}} + \frac{K_M}{j_{max} \cdot [H_2O_2]} \quad (4)$$

$$\frac{1}{j_{cat}} = \frac{1}{j_{max}} + \frac{K_M}{j_{max} \cdot [NO_2^-]} \quad (5)$$

where j_{cat} is the electrocatalytic current density and j_{max} is the maximum current density at substrate saturation. As the protein coverage of the DT SAM, Γ_0, differs for the investigated proteins (footnote *e* to Table 3), we have defined the maximum current density J_{max} normalized for Γ_0 values, namely $J_{max} = j_{max}/\Gamma_0$. Therefore, J_{max} values should reflect differences in k_{cat}, among the various species. Hence, the J_{max}/K_M ratio correspond to the catalytic efficiency of the adsorbed species[18,30,33,34,106]. The plots, shown in Figs. S7 and S8, yield the J_{max} and K_M values listed in Table 3.

As discussed previously for wt ycc on DT, we propose the following mechanism in which the 6th His ligand detaches from the iron(II) center [17,30]:

$$\text{cytFe(III)-His} + e \rightarrow \text{cytFe(II)}\cdots\text{His} \quad (6)$$

$$\text{cytFe(II)}\cdots\text{His} + H_2O_2 \rightarrow \text{cytFe(IV)=O (His)}_{\text{uncord}} + H_2O \quad (7)$$

$$\text{cytFe(IV)=O (His)}_{\text{uncoord}} + e + H_2O \rightarrow \text{cytFe(III)-His} + 2\ OH^- \quad (8)$$

while the mechanism for NO_2^- reduction for can be represented as [34,42]:

$$\text{cytFe(III)-His} + e \rightarrow \text{cytFe(II)}\cdots\text{His} \quad (9)$$

$$\text{cytFe(II)}\cdots\text{His} + NO_2^- + H_2O \rightarrow \text{cytFe(III)-His} + NO + 2\ OH^- \quad (10)$$

The kinetic affinities (K_M) of H_2O_2 for the heme iron of M80A and M80A/Y67A and their CL-adducts immobilized on DT are from one to three orders of magnitude larger [11] than those for immobilized horseradish peroxidase [107,108], hemoglobin variably immobilized on SAM-coated electrodes [109-111] and microperoxidase-11 [112,113]. Similarly, the K_M values for nitrite are three orders of magnitude greater than those for immobilized myoglobin [114] and cytochrome P450 [115] and comparable to that for freely diffusing nitrite reductase (NiR) accepting electrons from an electrode-immobilized cytochrome c_{551} [116].

The effects of point mutation(s) and CL binding on the electrocatalytic activity are reaction-specific. The changes can be better perceived at a glance thanks to the histograms shown in Fig. 8.

Table 3
Electrocatalytic activity toward hydrogen peroxide and nitrite reduction for wild-type *Saccharomyces cerevisiae* yeast *iso*-1-cytochrome *c* (ycc), its M80A and M80A/Y67A variants and their cardiolipin adducts (+CL) adsorbed on a gold electrode coated with decane-1-thiol.[a]

Substrate				K_M [d] (μM^{-1})	J_{max} [d,e] ($\mu A\ pmol^{-1}$)	J_{max}/K_M ($\mu A\ pmol^{-1}\mu M$)
H_2O_2	wt	DT[b]	free	4.10	0.65	0.158
			+ CL	4.91	1.06	0.216
		MUA/MU[c]	folded	n.a.		
			7 M urea	9.3	0.28	0.030
	M80A	DT	free	4.72	0.47	0.100
			+ CL	1.90	0.16	0.084
		MUA/MU[c]	folded	3.25	0.51	0.157
			7 M urea	1.38	0.30	0.217
	M80A/Y67A	DT	free	2.80	0.50	0.179
			+ CL	2.01	0.35	0.175
		MUA/MU[c]	folded	8.90	0.05	0.006
			7 M urea	5.36	0.25	0.047
NO_2^-	wt	DT	free	n.a.		
			+ CL			
		MUA/MU[c]	folded			
			7 M urea			
	M80A	DT	free	0.22	0.15	0.682
			+ CL	0.37	0.17	0.459
		MUA/MU[c]	folded	5.1	0.12	0.024
			7 M urea	0.64	0.19	0.297
	M80A/Y67A	DT	free	0.43	0.15	0.349
			+ CL	0.85	0.13	0.153
		MUA/MU[c]	folded	5.96	0.15	0.025
			7 M urea	4.51	0.22	0.049

[a] Working solution: 10 mM sodium perchlorate and 10 mM HEPES buffer at pH 7.2 T = 278 K.
[b] From ref. [17,18].
[c] From ref. [34].
[d] Average errors on K_M and J_{max} are ± 10% and ± 8% (relative error), respectively.
[e] J_{max} is the maximum catalytic current density normalized versus the Γ_0 values. Γ_0 = 15.6 (17.1), 8.0 (8.8) and 9.45 (10.4) pmoles cm^{-2} for ycc (CL), M80A (CL) and M80A/Y67A (CL).

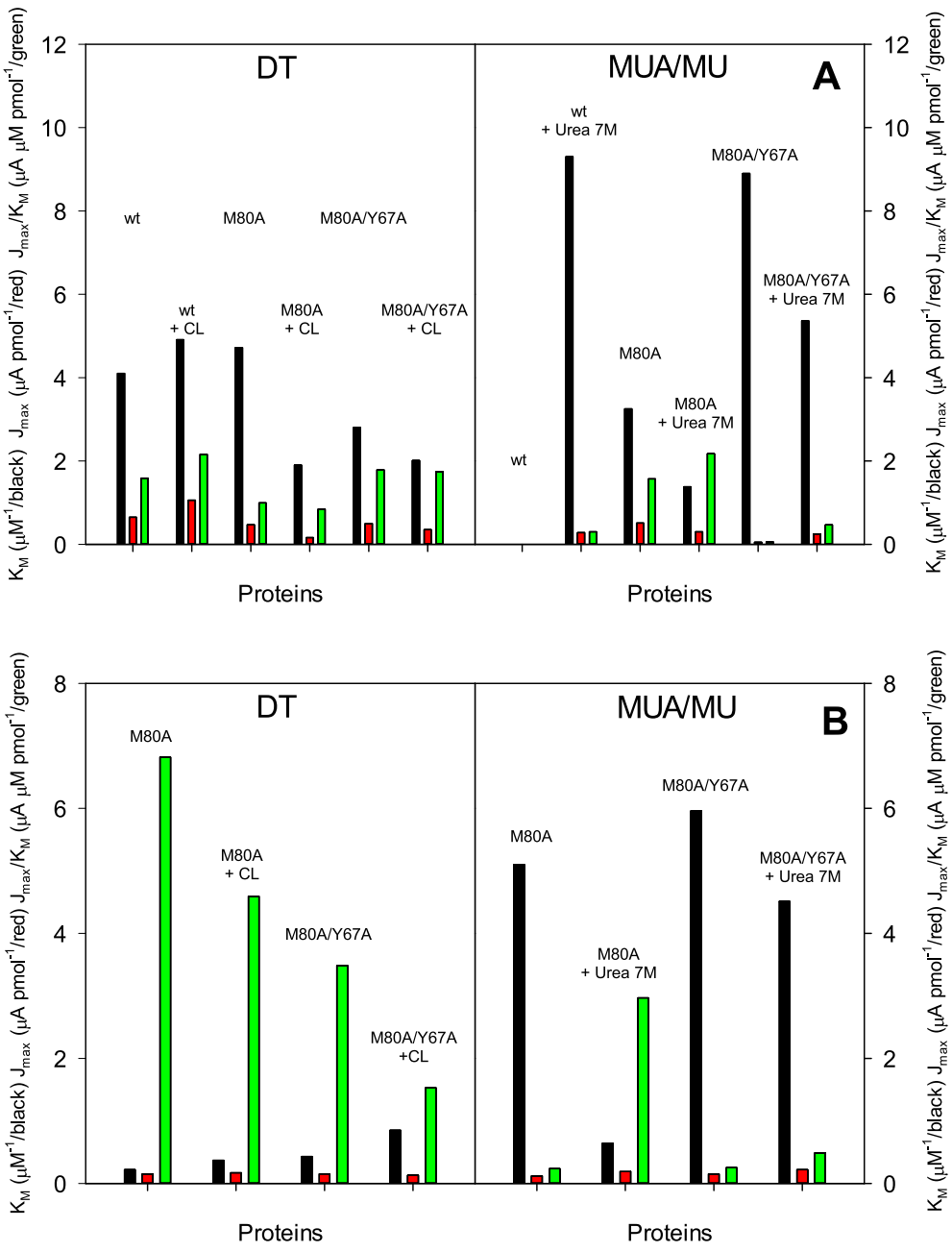

Fig. 8. Histograms depicting the K_M (μM^{-1}, black bar), J_{max} (μA $pmol^{-1}$, red bar) and $J_{max}/K_M \times 10$ (μA $pmol^{-1} \mu M$, green bar) values for the reductive electrocatalysis of A) H_2O_2 and B) NO_2^- carried out by wt *Saccharomyces cerevisiae* yeast *iso*-1 cytochrome and its M80A and M80A/Y67A variants immobilized on a gold electrode functionalized with a hydrophobic SAM of decane-1-thiol (DT) (this work) and a negatively charged SAM of MUA/MU (from ref.[17,34]) along with the corresponding adducts with cardiolipin (this work) and the same species in 7 M urea (from ref.[17,34]) immobilized under the same conditions. Fig. A (left frame, from left to right): wt; wt + CL; M80A; M80A + CL; M80A/Y67A; M80A/Y67A + CL. Fig. A (right frame, from left to right): wt; wt + Urea 7 M; M80A; M80A + Urea 7 M; M80A/Y67A; M80A/Y67A + Urea 7 M. Fig. B (left frame, from left to right): M80A; M80A + CL; M80A/Y67A; M80A/Y67A + CL. Fig. B (right frame, from left to right): M80A; M80A + Urea 7 M; M80A/Y67A; M80A/Y67A + Urea 7 M.

In particular, regarding the pseudoperoxidase reaction, M80A and M80A/Y67A show a slightly larger and a lower K_M value compared to wt, respectively. It is conceivable that the different hydrogen bonding network within the heme crevice for the two mutants (which we proposed above to affect also the kinetic constants for ET) disfavors H_2O_2 access to the heme iron in the former case and facilitates it in the latter. Likewise, due to the different structure and solvation properties of the heme environment, CL binding induces a K_M increase for wt and an opposite effect for both mutants. In the case of nitrite reduction, M80A mutation imparts the protein with activity (wt is inactive), while the additional Y67A mutation exerts an effect on K_M which is opposite to that observed toward H_2O_2 reduction. Analogously, CL-adduct formation increases K_M for both variants, opposite to the effect exerted on the pseudo peroxidase reaction. In this case, the increased hydrophobicity of the crevice would hinder access of the negatively charged nitrite ion to the heme center.

As we recently made an analogous study on the same species immobilized electrostatically onto the anionic MUA/MU SAM and subjected to urea-unfolding (see Table 3) [34], here we may compare the effects that different protein-SAM interactions exert on the same electrocatalytic reaction focusing on the J_{max}/K_M ratio (Fig. 8). It appears that wt ycc on DT is active as a catalyst for H_2O_2 reduction but it is not on MUA/MU [17,31,33,34] and is

unable to catalyze nitrite reduction on both surfaces [17,34,38]. Moreover, both variants are more catalytically active toward nitrite reduction on DT compared to MUA/MU (both folded and unfolded), while the pseudoperoxidase activity shows an opposite behavior.

This scenario indicates that the nature of the SAM strongly affects the ability of ycc to yield H_2O_2 and NO_2^- reductive electrocatalysis. We have found indeed that the intermolecular protein-SAM interactions affect heme iron axial coordination for wt (His/His on DT vs. His/Met on MUA/MU) and for M80A and M80A/Y67A (His/- and His/His in the reduced and oxidized state, respectively, on DT vs. His/OH^- on MUA/MU [34] in both redox states). This could explain the different pseudoperoxidase activity of wt ycc as the persistence of the Met-Fe(II) axial bond on MUA/MU hampers substrate binding, whereas the weaker and more labile His-Fe(II) bond on DT allows for substrate binding and turnover. Moreover, the different (most often opposed) nutation-induced activity changes for the same species immobilized on the two different SAMs subjected to the same point mutation confirm that protein-SAM interactions affect the H-bonding network, the polarity and the electrostatics of the heme environment besides the overall protein conformation, with an important role played by the solvation properties of the molecule.

4. Conclusions

Cytochrome *c* plays part of its physiological roles under conditions of motional restriction due to adsorption onto molecular constructs, as the inner mitochondrial membrane during the early events of apoptosis. In this and previous work, we have studied the properties and the reactivity of the heme center contained in the protein bound onto a SAM-coated surface in an electrochemical environment. As the cytc surface includes positively charged and hydrophobic patches, the SAMs of choice yielded a negative charge layer (MUA/MU) or a hydrophobic surface (DT), respectively. The present comparative study shows that the SAMs are not innocent and their action is not restricted to the protein surface but extends up to the heme center and its coordination and reactivity. The evidence presented here indicates that axial heme iron ligation, protein conformation, solvation properties, the reduction potentials for the Fe(III)/Fe(II) couples in the oxidation state-dependent conformers and the pseudoperoxidase and nitrite reductase activity of immobilized cytochrome *c* are all affected by the nature of the adsorbing surface, as well as changes due to point mutations and partial unfolding. Important effectors of the thermodynamics and kinetics of electron transfer and the equilibria among conformers under these conditions are solvent reorganization effects in the heme crevice and at the protein-SAM interface. We favor the idea that such response variability in relation to the different properties of the interacting surface contributes to the functional versatility and tunability of cytc in physiological conditions. Moreover, this study also points out that structural and reactivity data obtained for cytc subjected to a given surfacial adsorption, although defined as "non-denaturing", cannot be transferred to another even under the same conditions of medium composition and pH. This would also explain why the results in terms of the thermodynamics of the interaction and the structural changes in cytochrome *c* upon binding to different model membrane systems meant to mimic IMM are often at odds with each other. Hence, much care must be taken when transferring the information to the natural system.

Funding information

This work was supported by the University of Modena and Reggio Emilia FAR 2019 funding program.

Declaration of Competing Interest

The authors declare that they have no known competing financial interests or personal relationships that could have appeared to influence the work reported in this paper.

Acknowledgement

We thank dr. Diego Millo (ASML, Veldhoven, The Netherlands) for providing the original files of the SERRS spectra of wt ycc used in Fig. 5.

References

[1] D. Alvarez-Paggi, L. Hannibal, M.A. Castro, S. Oviedo-Rouco, V. Demicheli, V. Tórtora, F. Tomasina, R. Radi, D.H. Murgida, Multifunctional Cytochrome c: Learning New Tricks from an Old Dog, Chem. Rev. 117 (2017) 13382–13460, https://doi.org/10.1021/acs.chemrev.7b00257.

[2] R. Schweitzer-Stenner, Relating the multi-functionality of cytochrome c to membrane binding and structural conversion, Biophys. Rev. 10 (2018) 1151–1185, https://doi.org/10.1007/s12551-018-0409-4.

[3] L. Hannibal, F. Tomasina, D.A. Capdevila, V. Demicheli, V. Tórtora, D. Alvarez-Paggi, R. Jemmerson, D.H. Murgida, R. Radi, Alternative Conformations of Cytochrome c : Structure Function, and Detection, Biochemistry 55 (2016) 407–428, https://doi.org/10.1021/acs.biochem.5b01385.

[4] R. Schweitzer-Stenner, Cytochrome c: A Multifunctional Protein Combining Conformational Rigidity with Flexibility, New J. Sci. 2014 (2014) 1–28, https://doi.org/10.1155/2014/484538.

[5] P. Ascenzi, M. Coletta, M.T. Wilson, L. Fiorucci, M. Marino, F. Polticelli, F. Sinibaldi, R. Santucci, Cardiolipin-cytochrome c complex: Switching cytochrome c from an electron-transfer shuttle to a myoglobin- and a peroxidase-like heme-protein, IUBMB Life. 67 (2015) 98–109, https://doi.org/10.1002/iub.1350.

[6] V.E. Kagan, H.A. Bayir, N.A. Belikova, O. Kapralov, Y.Y. Tyurina, V.A. Tyurin, J. Jiang, D.A. Stoyanovsky, P. Wipf, P.M. Kochanek, J.S. Greenberger, B. Pitt, A.A. Shvedova, G. Borisenko, Cytochrome c/cardiolipin relations in mitochondria: a kiss of death, Free Radic. Biol. Med. 46 (2009) 1439–1453, https://doi.org/10.1016/j.freeradbiomed.2009.03.004.

[7] J. Muenzner, E.V. Pletneva, Structural transformations of cytochrome c upon interaction with cardiolipin, Chem. Phys. Lipids. 179 (2014) 57–63, https://doi.org/10.1016/j.chemphyslip.2013.11.002.

[8] J. Muenzner, J.R. Toffey, Y. Hong, E.V. Pletneva, Becoming a peroxidase: Cardiolipin-induced unfolding of cytochrome c, J. Phys. Chem. B. 117 (2013) 12878–12886, https://doi.org/10.1021/jp402104r.

[9] M. Hüttemann, P. Pecina, M. Rainbolt, T.H. Sanderson, V.E. Kagan, L. Samavati, J.W. Doan, I. Lee, The multiple functions of cytochrome c and their regulation in life and death decisions of the mammalian cell: From respiration to apoptosis, Mitochondrion. 11 (2011) 369–381, https://doi.org/10.1016/j.mito.2011.01.010.

[10] L.V. Basova, I.V. Kurnikov, L. Wang, V.B. Ritov, N.A. Belikova, I.I. Vlasova, A.A. Pacheco, D.E. Winnica, J. Peterson, H. Bayir, D.H. Waldeck, V.E. Kagan, Cardiolipin switch in mitochondria: Shutting off the reduction of cytochrome c and turning on the peroxidase activity, Biochemistry. 46 (2007) 3423–3434, https://doi.org/10.1021/bi061854k.

[11] A. Ranieri, C.A. Bortolotti, G. Di Rocco, G. Battistuzzi, M. Sola, M. Borsari, Electrocatalytic Properties of Immobilized Heme Proteins: Basic Principles and Applications, ChemElectroChem. 6 (2019) 5172–5185, https://doi.org/10.1002/celc.201901178.

[12] V. Yin, G.S. Shaw, L. Konermann, Cytochrome c as a Peroxidase: Activation of the Precatalytic Native State by H2O2-Induced Covalent Modifications, J. Am. Chem. Soc. 139 (2017) 15701–15709, https://doi.org/10.1021/jacs.7b07106.

[13] N. Tomášková, R. Varhač, V. Lysáková, A. Musatov, E. Sedlák, Peroxidase activity of cytochrome c in its compact state depends on dynamics of the heme region, Biochim. Biophys. Acta - Proteins Proteomics. 2018 (1866) 1073–1083, https://doi.org/10.1016/j.bbapap.2018.09.003.

[14] V.E. Kagan, V.A. Tyurin, J. Jiang, Y.Y. Tyurina, V.B. Ritov, A.A. Amoscato, A.N. Osipov, N.A. Belikova, A.A. Kapralov, V. Kini, I.I. Vlasova, Q. Zhao, M. Zou, P. Di, D.A. Svistunenko, I.V. Kurnikov, G.G. Borisenko, Cytochrome c acts as a cardiolipin oxygenase required for release of proapoptotic factors, Nat. Chem. Biol. 1 (2005) 223–232, https://doi.org/10.1038/nchembio727.

[15] F. Sinibaldi, L. Milazzo, B.D. Howes, M.C. Piro, L. Fiorucci, F. Polticelli, P. Ascenzi, M. Coletta, G. Smulevich, R. Santucci, The key role played by charge in the interaction of cytochrome c with cardiolipin, JBIC J. Biol. Inorg. Chem. 22 (2017) 19–29, https://doi.org/10.1007/s00775-016-1404-5.

[16] M.C. Piro, R. Santucci, E. Droghetti, F. Sinibaldi, L. Fiorucci, M. Coletta, D. Di Pierro, B.D. Howes, F. Polticelli, G. Smulevich, Role of Lysines in Cytochrome c –Cardiolipin Interaction, Biochemistry 52 (2013) 4578–4588, https://doi.org/10.1021/bi400324c.
[17] A. Ranieri, G. Di Rocco, D. Millo, G. Battistuzzi, C.A. Bortolotti, L. Lancellotti, M. Borsari, M. Sola, Thermodynamics and kinetics of reduction and species conversion at a hydrophobic surface for mitochondrial cytochromes c and their cardiolipin adducts, Electrochim. Acta. 176 (2015) 1019–1028, https://doi.org/10.1016/j.electacta.2015.07.065.
[18] A. Ranieri, D. Millo, G. Di Rocco, G. Battistuzzi, C.A. Bortolotti, M. Borsari, M. Sola, Immobilized cytochrome c bound to cardiolipin exhibits peculiar oxidation state-dependent axial heme ligation and catalytically reduces dioxygen, JBIC J. Biol. Inorg. Chem. 20 (2015) 531–540, https://doi.org/10.1007/s00775-015-1238-6.
[19] A. Díaz-Quintana, G. Pérez-Mejías, A. Guerra-Castellano, M.A. De la Rosa, I. Díaz-Moreno, Wheel and Deal in the Mitochondrial Inner Membranes: The Tale of Cytochrome c and Cardiolipin, Oxid. Med. Cell. Longev. 2020 (2020) 1–20, https://doi.org/10.1155/2020/6813405.
[20] A. Paradisi, M. Bellei, L. Paltrinieri, C.A. Bortolotti, G. Di Rocco, A. Ranieri, M. Borsari, M. Sola, G. Battistuzzi, Binding of S. cerevisiae iso-1 cytochrome c and its surface lysine-to-alanine variants to cardiolipin: charge effects and the role of the lipid to protein ratio, JBIC, J. Biol. Inorg. Chem. 25 (2020) 467–487, https://doi.org/10.1007/s00775-020-01776-1.
[21] J. Hanske, J.R. Toffey, A.M. Morenz, A.J. Bonilla, K.H. Schiavoni, E.V. Pletneva, Conformational properties of cardiolipin-bound cytochrome c, Proc. Natl. Acad. Sci. 109 (2011) 125–130, https://doi.org/10.1073/pnas.1112312108.
[22] B. Milorey, R. Schweitzer-Stenner, R. Kurbaj, D. Malyshka, pH-Induced Switch between Different Modes of Cytochrome c Binding to Cardiolipin-Containing Liposomes, ACS Omega. 4 (2019) 1386–1400, https://doi.org/10.1021/acsomega.8b02574.
[23] L.C. Godoy, C. Muñoz-Pinedo, L. Castro, S. Cardaci, C.M. Schonhoff, M. King, V. Tórtora, M. Marín, Q. Miao, J.F. Jiang, A. Kapralov, R. Jemmerson, G.G. Silkstone, J.N. Patel, J.E. Evans, M.T. Wilson, D.R. Green, V.E. Kagan, R. Radi, J.B. Mannick, Disruption of the M80-Fe ligation stimulates the translocation of cytochrome c to the cytoplasm and nucleus in nonapoptotic cells, Proc. Natl. Acad. Sci. 106 (2009) 2653–2658, https://doi.org/10.1073/pnas.0809279106.
[24] D.A. Capdevila, S. Oviedo Rouco, F. Tomasina, V. Tortora, V. Demicheli, R. Radi, D.H. Murgida, Active Site Structure and Peroxidase Activity of Oxidatively Modified Cytochrome c Species in Complexes with Cardiolipin, Biochemistry. 54 (2015) 7491–7504, https://doi.org/10.1021/acs.biochem.5b00922.
[25] D.A. Capdevila, W.A. Marmisollé, F. Tomasina, V. Demicheli, M. Portela, R. Radi, D.H. Murgida, Specific methionine oxidation of cytochrome c in complexes with zwitterionic lipids by hydrogen peroxide: Potential implications for apoptosis, Chem. Sci. 6 (2015) 705–713, https://doi.org/10.1039/c4sc02181a.
[26] A.A. Kapralov, N. Yanamala, Y.Y. Tyurina, L. Castro, A. Samhan-Arias, Y.A. Vladimirov, A. Maeda, A.A. Weitz, J. Peterson, D. Mylnikov, V. Demicheli, V. Tortora, J. Klein-Seetharaman, R. Radi, V.E. Kagan, Topography of tyrosine residues and their involvement in peroxidation of polyunsaturated cardiolipin in cytochrome c/cardiolipin peroxidase complexes, Biochim. Biophys. Acta - Biomembr. 2011 (1808) 2147–2155, https://doi.org/10.1016/j.bbamem.2011.04.009.
[27] K. González-Arzola, A. Díaz-Quintana, F. Rivero-Rodríguez, A. Velázquez-Campoy, M.A. De La Rosa, I. Díaz-Moreno, Histone chaperone activity of Arabidopsis thaliana NRP1 is blocked by cytochrome c, Nucleic Acids Res. 45 (2017) 2150–2165, https://doi.org/10.1093/nar/gkw1215.
[28] K. González-Arzola, I. Díaz-Moreno, A. Cano-González, A. Díaz-Quintana, A. Velázquez-Campoy, B. Moreno-Beltrán, A. López-Rivas, M.A. De La Rosa, A.R. Fersht, Structural basis for inhibition of the histone chaperone activity of SET/TAF-Iβ by cytochrome c, Proc. Natl. Acad. Sci. U. S. A. 112 (2015) 9908–9913, https://doi.org/10.1073/pnas.1508040112.
[29] S. Monari, D. Millo, A. Ranieri, G. Di Rocco, G. van der Zwan, C. Gooijer, S. Peressini, C. Tavagnacco, P. Hildebrandt, M. Borsari, The impact of urea-induced unfolding on the redox process of immobilised cytochrome c, JBIC J. Biol. Inorg. Chem. 15 (2010) 1233–1242, https://doi.org/10.1007/s00775-010-0681-7.
[30] A. Ranieri, G. Battistuzzi, M. Borsari, C.A. Bortolotti, G. Di Rocco, S. Monari, M. Sola, A bis-histidine-ligated unfolded cytochrome c immobilized on anionic SAM shows pseudo-peroxidase activity, Electrochem. Commun. 14 (2012) 29–31, https://doi.org/10.1016/j.elecom.2011.10.021.
[31] C.A. Bortolotti, L. Paltrinieri, S. Monari, A. Ranieri, M. Borsari, G. Battistuzzi, M. Sola, A surface-immobilized cytochrome c variant provides a pH-controlled molecular switch, Chem. Sci. 3 (2012) 807–810, https://doi.org/10.1039/C1SC00821H.
[32] G. Di Rocco, A. Ranieri, C.A. Bortolotti, G. Battistuzzi, A. Bonifacio, V. Sergo, M. Borsari, M. Sola, Axial iron coordination and spin state change in a heme c upon electrostatic protein–SAM interaction, Phys. Chem. Chem. Phys. 15 (2013) 13499, https://doi.org/10.1039/c3cp50222h.
[33] A. Ranieri, C.A. Bortolotti, G. Battistuzzi, M. Borsari, L. Paltrinieri, G. Di Rocco, M. Sola, Effect of motional restriction on the unfolding properties of a cytochrome c featuring a His/Met-His/His ligation switch, Metallomics. 6 (2014) 874–884, https://doi.org/10.1039/c3mt00311f.
[34] L. Lancellotti, M. Borsari, M. Bellei, A. Bonifacio, C.A. Bortolotti, G. Di Rocco, A. Ranieri, M. Sola, G. Battistuzzi, Unpublished results, (n.d.).
[35] N.A. Belikova, Y.A. Vladimirov, A.N. Osipov, A.A. Kapralov, V.A. Tyurin, M.V. Potapovich, L.V. Basova, J. Peterson, I.V. Kurnikov, V.E. Kagan, Peroxidase Activity and Structural Transitions of Cytochrome c Bound to Cardiolipin-Containing Membranes, Biochemistry. 45 (2006) 4998–5009, https://doi.org/10.1021/bi0525573.
[36] B.S. Rajagopal, A.N. Edzuma, M.A. Hough, K.L.I.M. Blundell, V.E. Kagan, A.A. Kapralov, L.A. Fraser, J.N. Butt, G.G. Silkstone, M.T. Wilson, D.A. Svistunenko, J. A.R. Worrall, The hydrogen-peroxide-induced radical behaviour in human cytochrome c –phospholipid complexes: implications for the enhanced pro-apoptotic activity of the G41S mutant, Biochem. J. 456 (2013) 441–452, https://doi.org/10.1042/bj20130758.
[37] M. Li, A. Mandal, V.A. Tyurin, M. DeLucia, J. Ahn, V.E. Kagan, P.C.A. van der Wel, Surface-Binding to Cardiolipin Nanodomains Triggers Cytochrome c Pro-apoptotic Peroxidase Activity via Localized Dynamics, Structure. (2019) 1–11, https://doi.org/10.1016/j.str.2019.02.007.
[38] S. Casalini, G. Battistuzzi, M. Borsari, C.A. Bortolotti, G. Di Rocco, A. Ranieri, M. Sola, Electron transfer properties and hydrogen peroxide electrocatalysis of cytochrome c variants at positions 67 and 80, J. Phys. Chem. B. 114 (2010) 1698–1706, https://doi.org/10.1021/jp9090365.
[39] C.A. Bortolotti, G. Battistuzzi, M. Borsari, P. Facci, A. Ranieri, M. Sola, The Redox Chemistry of the Covalently Immobilized Native and Low-pH Forms of Yeast Iso-1-cytochrome c, J. Am. Chem. Soc. 128 (2006) 5444–5451, https://doi.org/10.1021/ja0573662.
[40] S. Monari, G. Battistuzzi, C. Dennison, M. Borsari, A. Ranieri, M.J. Siwek, M. Sola, Factors affecting the electron transfer properties of an immobilized cupredoxin, J. Phys. Chem. C. 114 (2010) 22322–22329, https://doi.org/10.1021/jp110096a.
[41] E. Castellini, C.A. Bortolotti, G. Di Rocco, F. Bernini, A. Ranieri, Enhancing Biocatalysis: The Case of Unfolded Cytochrome c Immobilized on Kaolinite, ChemCatChem. 5 (2013) 1765–1768, https://doi.org/10.1002/cctc.201200876.
[42] S. Casalini, G. Battistuzzi, M. Borsari, A. Ranieri, M. Sola, Catalytic reduction of dioxygen and nitrite ion at a Met80Ala cytochrome c-functionalized electrode, J. Am. Chem. Soc. 130 (2008) 15099–15104, https://doi.org/10.1021/ja8040724.
[43] S. Casalini, G. Battistuzzi, M. Borsari, C.A. Bortolotti, A. Ranieri, M. Sola, Electron transfer and electrocatalytic properties of the immobilized Methionine80Alanine cytochrome c variant, J. Phys. Chem. B. 112 (2008) 1555–1563, https://doi.org/10.1021/jp0765953.
[44] G. Battistuzzi, C.A. Bortolotti, M. Bellei, G. Di Rocco, J. Salewski, P. Hildebrandt, M. Sola, Role of Met80 and Tyr67 in the Low-pH Conformational Equilibria of Cytochrome c, Biochemistry. 51 (2012) 5967–5978, https://doi.org/10.1021/bi3007302.
[45] A. Ranieri, G. Battistuzzi, M. Borsari, C.A. Bortolotti, G. Di Rocco, M. Sola, pH and Solvent H/D Isotope Effects on the Thermodynamics and Kinetics of Electron Transfer for Electrode-Immobilized Native and Urea-Unfolded Stellacyanin, Langmuir. 28 (2012) 15087–15094, https://doi.org/10.1021/la303363h.
[46] S. Monari, G. Battistuzzi, C.A. Bortolotti, S. Yanagisawa, K. Sato, C. Li, I. Salard, D. Kostrz, M. Borsari, A. Ranieri, C. Dennison, M. Sola, Understanding the mechanism of short-range electron transfer using an immobilized cupredoxin, J. Am. Chem. Soc. 134 (2012) 11848–11851, https://doi.org/10.1021/ja303425b.
[47] J.M. Bradley, G. Silkstone, M.T. Wilson, M.R. Cheesman, J.N. Butt, Probing a complex of cytochrome c and cardiolipin by magnetic circular dichroism spectroscopy: Implications for the initial events in apoptosis, J. Am. Chem. Soc. 133 (2011) 19676–19679, https://doi.org/10.1021/ja209144h.
[48] I. Husu, S. Kapetanaki, G. Silkstone, U. Liebl, M.T. Wilson, M. Vos, Interaction of CO/NO with the Apoptosis-Inducing Cytochrome C -Cardiolipin Complex, Biophys. J. 98 (2010) 631a, https://doi.org/10.1016/j.bpj.2009.12.3455.
[49] G. Battistuzzi, M. Borsari, C.A. Bortolotti, G. Di Rocco, A. Ranieri, M. Sola, Effects of mutational (Lys to Ala) surface charge changes on the redox properties of electrode-immobilized cytochrome c, J. Phys. Chem. B. 111 (2007) 10281–10287, https://doi.org/10.1021/jp0730343.
[50] N. Osheroff, D.L. Brautigan, E. Margoliash, Mapping of anion binding sites on cytochrome c by differential chemical modification of lysine residues, Proc. Natl. Acad. Sci. U. S. A. 77 (1980) 4439–4443, https://doi.org/10.1073/pnas.77.8.4439.
[51] G. Battistuzzi, M. Borsari, D. Dallari, I. Lancellotti, M. Sola, Anion binding to mitochondrial cytochromes c studied through electrochemistry. Effects of the neutralization of surface charges on the redox potential, Eur. J. Biochem. 241 (1996) 208–214, https://doi.org/10.1111/j.1432-1033.1996.0208t.x.
[52] G. Battistuzzi, M. Borsari, M. Sola, Anion binding to cytochrome c2: Implications on protein-ion interactions in class I cytochromes c, Arch. Biochem. Biophys. 339 (1997) 283–290, https://doi.org/10.1006/abbi.1996.9862.
[53] L. Milazzo, L. Tognaccini, B.D. Howes, F. Sinibaldi, M.C. Piro, M. Fittipaldi, M.C. Baratto, R. Pogni, R. Santucci, G. Smulevich, Unravelling the Non-Native Low-Spin State of the Cytochrome c-Cardiolipin Complex: Evidence of the Formation of a His-Ligated Species Only, Biochemistry. 56 (2017) 1887–1898, https://doi.org/10.1021/acs.biochem.6b01281.
[54] E.J. Snider, J. Muenzner, J.R. Toffey, Y. Hong, E.V. Pletneva, Multifaceted Effects of ATP on Cardiolipin-Bound Cytochrome c, Biochemistry. 52 (2013) 993–995, https://doi.org/10.1021/bi301682c.
[55] F. Sinibaldi, B.D. Howes, M.C. Piro, F. Polticelli, C. Bombelli, T. Ferri, M. Coletta, G. Smulevich, R. Santucci, Extended cardiolipin anchorage to cytochrome c: A model for protein-mitochondrial membrane binding, J. Biol. Inorg. Chem. 15 (2010) 689–700, https://doi.org/10.1007/s00775-010-0636-z.

[56] G. Battistuzzi, M. Borsari, D. Dallari, S. Ferretti, M. Sola, Cyclic Voltammetry and ^{1}H-NMR of Rhodopseudomonas palustris Cytochrome c_2 Probing Surface Charges through Anion-Binding Studies, Eur. J. Biochem. 233 (1995) 335–339, https://doi.org/10.1111/j.1432-1033.1995.335_1.x.

[57] A.J. Bard, L.R. Faulkner, Electrochemical Methods Fundamentals and Applications, 2nd ed., JOHN WILEY & SONS, INC., New York, 2001. https://www.wiley.com/en-it/Electrochemical+Methods%3A+Fundamentals+and+Applications%2C+2nd+Edition-p-9780471043720.

[58] E.L. Yee, M.J. Weaver, Functional dependence upon ligand composition of the reaction entropies for some transition-metal redox couples containing mixed ligands, Inorg. Chem. 19 (1980) 1077–1079, https://doi.org/10.1021/ic50206a063.

[59] E.L. Yee, R.J. Cave, K.L. Guyer, T.P. D., M.J. Weaver, A survey of ligand effects upon the reaction entropies of some transition metal redox couples, J. Am. Chem. Soc. 101 (1979) 1131–1137. doi:10.1021/ja00499a013.

[60] V.T. Taniguchi, N. Sailasuta—Scott, F.C. Anson, H.B. Gray, Thermodynamics of Metalloprotein Electron Transfer Reactions, Pure Appl. Chem. 52 (1980) 2275—2281. doi:0033—4545/80/1001—2275.

[61] G. Battistuzzi, M. Borsari, M. Sola, F. Francia, Redox Thermodynamics of the Native and Alkaline Forms of Eukaryotic and Bacterial Class I Cytochromes c †, Biochemistry. 36 (1997) 16247–16258, https://doi.org/10.1021/bi971535g.

[62] G. Battistuzzi, M. Borsari, L. Loschi, M. Sola, Redox thermodynamics, acid-base equilibria and salt-induced effects for the cucumber basic protein. General implications for blue-copper proteins, JBIC J. Biol. Inorg. Chem. 2 (1997) 350–359, https://doi.org/10.1007/s007750050142.

[63] G. Battistuzzi, M. Borsari, L. Loschi, F. Righi, M. Sola, Redox Thermodynamics of Blue Copper Proteins, J. Am. Chem. Soc. 121 (1999) 501–506, https://doi.org/10.1021/ja982126q.

[64] G. Battistuzzi, M. Borsari, M. Sola, Medium and Temperature Effects on the Redox Chemistry of Cytochrome c, Eur. J. Inorg. Chem. 2001 (2001) 2989, https://doi.org/10.1002/1099-0682(200112)2001:12<2989::aid-ejic2989>3.3.co;2-5.

[65] E. Laviron, General expression of the linear potential sweep voltammogram in the case of diffusionless electrochemical systems, J. Electroanal. Chem. 101 (1979) 19–28, https://doi.org/10.1016/S0022-0728(79)80075-3.

[66] D. Britz, iR Elimination in Electrochemical Cells, J. Electroanal. Chem., 88 309–352. 88 (1978) 309–353. https://pdf.sciencedirectassets.com/280368/1-s2.0-S0022072878X81228/1-s2.0-S0022072878801223/main.pdf?X-Amz-Security-Token=IQoJb3JpZ2luX2VjEDIaCXVzLWVhc3QtMSJIMEYCIQDXVdH5bScWK8VWPo%252BamX1L0fKly45SqsBPKxbUMhY%252BOgIhAK%252B9P7sgEQ7wc7kQHFL8qviUaKsOjiUy.

[67] A. Bonifacio, D. Millo, C. Gooijer, R. Boegschoten, G. van der Zwan, Linearly Moving Low-Volume Spectroelectrochemical Cell for Microliter-Scale Surface-Enhanced Resonance Raman Spectroscopy of Heme Proteins, Anal. Chem. 76 (2004) 1529–1531, https://doi.org/10.1021/ac0350615.

[68] D. Millo, A. Ranieri, W. Koot, C. Gooijer, G. van der Zwan, Towards Combined Electrochemistry and Surface-Enhanced Resonance Raman of Heme Proteins: Improvement of Diffusion Electrochemistry of Cytochrome c at Silver Electrodes Chemically Modified with 4-Mercaptopyridine, Anal. Chem. 78 (2006) 5622–5625, https://doi.org/10.1021/ac060807v.

[69] L. Banci, I. Bertini, K.L. Bren, H.B. Gray, P. Turano, pH-dependent equilibria of yeast Met80Ala-iso-1-cytochrome c probed by NMR spectroscopy: a comparison with the wild-type protein, Chem. Biol. 2 (1995) 377–383, https://doi.org/10.1016/1074-5521(95)90218-X.

[70] K.L. Bren, H.B. Gray, Structurally engineered cytochromes with novel ligand-binding sites: oxy and carbon monoxy derivatives of semisynthetic horse heart Ala80 cytochrome c, J. Am. Chem. Soc. 115 (1993) 10382–10383, https://doi.org/10.1021/ja00075a073.

[71] Y. Lu, D.R. Casimiro, K.L. Bren, J.H. Richards, H.B. Gray, Structurally engineered cytochromes with unusual ligand-binding properties: expression of Saccharomyces cerevisiae Met-80 → Ala iso-1-cytochrome c, Proc. Natl. Acad. Sci. 90 (1993) 11456–11459, https://doi.org/10.1073/pnas.90.24.11456.

[72] S. Oellerich, H. Wackerbarth, P. Hildebrandt, Conformational equilibria and dynamics of cytochrome c induced by binding of sodium dodecyl sulfate monomers and micelles, Eur. Biophys. J. 32 (2003) 599–613, https://doi.org/10.1007/s00249-003-0306-y.

[73] M. Simon, V. Metzinger-Le Meuth, S. Chevance, O. Delalande, A. Bondon, Versatility of non-native forms of human cytochrome c: pH and micellar concentration dependence, JBIC, J. Biol. Inorg. Chem. 18 (2013) 27–38, https://doi.org/10.1007/s00775-012-0946-4.

[74] S. Oellerich, H. Wackerbarth, P. Hildebrandt, Spectroscopic characterization of nonnative conformational states of cytochrome c, J. Phys. Chem. B. 106 (2002) 6566–6580, https://doi.org/10.1021/jp013841g.

[75] G. Battistuzzi, M. Borsari, F. De Rienzo, G. Di Rocco, A. Ranieri, M. Sola, Free Energy of Transition for the Individual Alkaline Conformers of Yeast Iso-1-cytochrome c, Biochemistry. 46 (2007) 1694–1702, https://doi.org/10.1021/bi061961e.

[76] G. Battistuzzi, M. Bellei, C. Dennison, G. Di Rocco, K. Sato, M. Sola, S. Yanagisawa, Thermodynamics of the alkaline transition in phytocyanins, JBIC J. Biol. Inorg. Chem. 12 (2007) 895–900, https://doi.org/10.1007/s00775-007-0245-7.

[77] E.B. Starikov, Valid entropy – enthalpy compensation : Fine mechanisms at microscopic level, Chem. Phys. Lett. 564 (2013) 88–92, https://doi.org/10.1016/j.cplett.2013.02.016.

[78] E.B. Starikov, B. Norde, Enthalpy - Entropy Compensation, A Phantom or Something Useful? (2007) 14431–14435.

[79] E.B. Starikov, B. Nordén, Entropy–enthalpy compensation as a fundamental concept and analysis tool for systematical experimental data, Chem. Phys. Lett. 538 (2012) 118–120, https://doi.org/10.1016/j.cplett.2012.04.028.

[80] L. Movileanu, E.A. Schiff, Entropy–enthalpy compensation of biomolecular systems in aqueous phase: a dry perspective, Monatshefte Für Chemie - Chem. Mon. 144 (2013) 59–65, https://doi.org/10.1007/s00706-012-0839-9.

[81] G. Battistuzzi, M. Borsari, G.W. Canters, E. De Waal, A. Leonardi, A. Ranieri, M. Sola, Thermodynamics of the acid transition in blue copper proteins, Biochemistry. 41 (2002) 14293–14298, https://doi.org/10.1021/bi026564s.

[82] J. Vlasits, M. Bellei, C. Jakopitsch, F. De Rienzo, P.G. Furtmüller, M. Zamocky, M. Sola, G. Battistuzzi, C. Obinger, Disruption of the H-bond network in the main access channel of catalase-peroxidase modulates enthalpy and entropy of Fe(III) reduction, J. Inorg. Biochem. 104 (2010) 648–656, https://doi.org/10.1016/j.jinorgbio.2010.02.006.

[83] M. Bellei, G. Battistuzzi, S. pao Wu, S.S. Mansy, J.A. Cowan, M. Sola, Control of reduction thermodynamics in [2Fe-2S] ferredoxins. Entropy-enthalpy compensation and the influence of surface mutations, J. Inorg. Biochem. 104 (2010) 691–696, https://doi.org/10.1016/j.jinorgbio.2010.03.001.

[84] S. Monari, A. Ranieri, G. Di Rocco, G. van der Zwan, S. Peressini, C. Tavagnacco, D. Millo, M. Borsari, Redox thermodynamics of cytochromes c subjected to urea induced unfolding, J. Appl. Electrochem. 39 (2009) 2181–2190, https://doi.org/10.1007/s10800-009-9804-7.

[85] G. Battistuzzi, M. Bellei, M. Borsari, G.W. Canters, E. De Waal, L.J.C. Jeuken, A. Ranieri, M. Sola, Control of metalloprotein reduction potential: Compensation phenomena in the reduction thermodynamics of blue copper proteins, Biochemistry. 42 (2003) 9214–9220, https://doi.org/10.1021/bi034585w.

[86] G. Battistuzzi, M. Borsari, G. Di Rocco, A. Ranieri, M. Sola, Enthalpy/entropy compensation phenomena in the reduction thermodynamics of electron transport metalloproteins, JBIC J. Biol. Inorg. Chem. 9 (2004) 23–26, https://doi.org/10.1007/s00775-003-0490-3.

[87] S. Monari, A. Ranieri, C.A. Bortolotti, S. Peressini, C. Tavagnacco, M. Borsari, Unfolding of cytochrome c immobilized on self-assembled monolayers. An electrochemical study, Electrochim. Acta. 56 (2011) 6925–6931, https://doi.org/10.1016/j.electacta.2011.06.022.

[88] E. Grunwald, C. Steel, Solvent Reorganization and Thermodynamic Enthalpy-Entropy Compensation, J. Am. Chem. Soc. 117 (1995) 5687–5692, https://doi.org/10.1021/ja00126a009.

[89] E. Grunwald, Thermodynamic properties of nonpolar solutes in water and the structure of hydrophobic hydration shells, J. Am. Chem. Soc. 108 (1986) 5726–5731, https://doi.org/10.1021/ja00279a011.

[90] L. Liu, Q.-X. Guo, Isokinetic Relationship, Isoequilibrium Relationship, and Enthalpy−Entropy Compensation, Chem. Rev. 101 (2001) 673–696, https://doi.org/10.1021/cr990416z.

[91] G. McNay, D. Eustace, W.E. Smith, K. Faulds, D. Graham, Surface-enhanced Raman scattering (SERS) and surface-enhanced resonance raman scattering (SERRS): A review of applications, Appl. Spectrosc. 65 (2011) 825–837, https://doi.org/10.1366/11-06365.

[92] A. Procyk, D.F. Bocian, Vibrational Characteristics of Tetrapyrrolic Macrocycles, Annu. Rev. Phys. Chem. 43 (1992) 465–496, https://doi.org/10.1146/annurev.physchem.43.1.465.

[93] T. Spiro, L. X, eds., Biological applications of Raman spectroscopy, Wiley, New York, 1990.

[94] M. Abe, T. Kitagawa, Y. Kyogoku, Resonance Raman spectra of octaethylporphyrinato-Ni(II) and meso-deuterated and 15N substituted derivatives. II. A normal coordinate analysis, J. Chem. Phys. 69 (1978) 4526–4534, https://doi.org/10.1063/1.436450.

[95] Y. Hong, J. Muenzner, S.K. Grimm, E.V. Pletneva, Origin of the conformational heterogeneity of cardiolipin-bound cytochrome c, J. Am. Chem. Soc. 134 (2012) 18713–18723, https://doi.org/10.1021/ja307426k.

[96] P. Ascenzi, D. Sbardella, F. Sinibaldi, R. Santucci, M. Coletta, The nitrite reductase activity of horse heart carboxymethylated-cytochrome c is modulated by cardiolipin, JBIC J. Biol. Inorg. Chem. 21 (2016) 421–432, https://doi.org/10.1007/s00775-016-1351-1.

[97] S. Prasad, N.C. Maiti, S. Mazumdar, S. Mitra, Reaction of hydrogen peroxide and peroxidase activity in carboxymethylated cytochrome c: spectroscopic and kinetic studies, Biochim. Biophys. Acta - Protein Struct. Mol. Enzymol. (1596 (2002)) 63–75, https://doi.org/10.1016/S0167-4838(02)00205-4.

[98] L.K. Lightning, H.W. Huang, P. Moënne-Loccoz, T.M. Loehr, D.J. Schuller, T.L. Poulos, P.R. Ortiz De Montellano, Disruption of an Active Site Hydrogen Bond Converts Human Heme Oxygenase-1 into a Peroxidase, J. Biol. Chem. 276 (2001) 10612–10619, https://doi.org/10.1074/jbc.M010349200.

[99] C. Tavagnacco, S. Monari, A. Ranieri, C.A. Bortolotti, S. Peressini, M. Borsari, Immobilized unfolded cytochrome c acts as a catalyst for dioxygen reduction, Chem. Commun. 47 (2011) 11122–11124, https://doi.org/10.1039/C1CC13854E.

[100] V.E. Kagan, Y.Y. Tyurina, H. Bayir, C.T. Chu, A.A. Kapralov, I.I. Vlasova, N.A. Belikova, V.A. Tyurin, A. Amoscato, M. Epperly, J. Greenberger, S. DeKosky, A. A. Shvedova, J. Jiang, The "pro-apoptotic genies" get out of mitochondria: Oxidative lipidomics and redox activity of cytochrome c/cardiolipin complexes, Chem. Biol. Interact. 163 (2006) 15–28, https://doi.org/10.1016/j.cbi.2006.04.019.

[101] S. Song, R.A. Clark, E.F. Bowden, M.J. Tarlov, Characterization of cytochrome c/alkanethiolate structures prepared by self-assembly on gold, J. Phys. Chem. 97 (1993) 6564–6572, https://doi.org/10.1021/j100126a037.

[102] M.J. Tarlov, E.F. Bowden, Electron-transfer reaction of cytochrome c adsorbed on carboxylic acid terminated alkanethiol monolayer electrodes, J. Am. Chem. Soc. 113 (1991) 1847–1849, https://doi.org/10.1021/ja00005a068.
[103] T.M. Nahir, R.A. Clark, E.F. Bowden, Linear-Sweep Voltammetry of Irreversible Electron Transfer in Surface-Confined Species Using the Marcus Theory, Anal. Chem. 66 (1994) 2595–2598, https://doi.org/10.1021/ac00087a027.
[104] R.A. Marcus, N. Sutin, Electron transfers in chemistry and biology, Biochim. Biophys. Acta - Rev. Bioenerg. 811 (1985) 265–322, https://doi.org/10.1016/0304-4173(85)90014-X.
[105] R.A. Kamin, G.S. Wilson, Rotating ring-disk enzyme electrode for biocatalysis kinetic studies and characterization of the immobilized enzyme layer, Anal. Chem. 52 (1980) 1198–1205, https://doi.org/10.1021/ac50058a010.
[106] S. Monari, G. Battistuzzi, M. Borsari, G. Di Rocco, L. Martini, A. Ranieri, M. Sola, Heterogeneous Electron Transfer of a Two-Centered Heme Protein: Redox and Electrocatalytic Properties of Surface-Immobilized Cytochrome c 4, J. Phys. Chem. B. 113 (2009) 13645–13653, https://doi.org/10.1021/jp906339u.
[107] J. Li, S.N. Tan, H. Ge, Silica sol-gel immobilized amperometric biosensor for hydrogen peroxide, Anal. Chim. Acta. 335 (1996) 137–145, https://doi.org/10.1016/S0003-2670(96)00337-6.
[108] X. Yi, J. Huang-Xian, C. Hong-Yuan, Direct Electrochemistry of Horseradish Peroxidase Immobilized on a Colloid/Cysteamine-Modified Gold Electrode, Anal. Biochem. 278 (2000) 22–28, https://doi.org/10.1006/abio.1999.4360.
[109] R. Huang, N. Hu, Direct electrochemistry and electrocatalysis with horseradish peroxidase in Eastman AQ films, Bioelectrochemistry. 54 (2001) 75–81, https://doi.org/10.1016/S1567-5394(01)00113-X.
[110] C. Fan, H. Wang, S. Sun, D. Zhu, G. Wagner, G. Li, Electron-Transfer Reactivity and Enzymatic Activity of Hemoglobin in a SP Sephadex Membrane, Anal. Chem. 73 (2001) 2850–2854, https://doi.org/10.1021/ac001397s.
[111] Z. Tong, R. Yuan, Y. Chai, S. Chen, Y. Xie, Amperometric biosensor for hydrogen peroxide based on Hemoglobin/DNA/Poly-2,6-pyridinediamine modified gold electrode, Thin Solid Films. 515 (2007) 8054–8058, https://doi.org/10.1016/j.tsf.2007.04.051.
[112] W. Huang, J. Jia, Z. Zhang, X. Han, J. Tang, J. Wang, S. Dong, E. Wang, Hydrogen peroxide biosensor based on microperoxidase-11 entrapped in lipid membrane, Biosens. Bioelectron. 18 (2003) 1225–1230, https://doi.org/10.1016/S0956-5663(03)00070-8.
[113] A.N.J. Moore, E. Katz, I. Willner, Electrocatalytic reduction of organic peroxides in organic solvents by microperoxidase-11 immobilized as a monolayer on a gold electrode, J. Electroanal. Chem. 417 (1996) 189–192, https://doi.org/10.1016/S0022-0728(96)04736-5.
[114] R. Lin, M. Bayachou, J. Greaves, P.J. Farmer, Nitrite Reduction by Myoglobin in Surfactant Films, J. Am. Chem. Soc. 119 (1997) 12689–12690, https://doi.org/10.1021/ja972529a.
[115] C.E. Immoos, J. Chou, M. Bayachou, E. Blair, J. Greaves, P.J. Farmer, Electrocatalytic Reductions of Nitrite, Nitric Oxide, and Nitrous Oxide by Thermophilic Cytochrome P450 CYP119 in Film-Modified Electrodes and an Analytical Comparison of Its Catalytic Activities with Myoglobin, J. Am. Chem. Soc. 126 (2004) 4934–4942, https://doi.org/10.1021/ja038925c.
[116] E. Lojou, F. Cutruzzolà, M. Tegoni, P. Bianco, F. Cutruzzola, M. Tegoni, P. Bianco, Electrochemical study of the intermolecular electron transfer to Pseudomonas aeruginosa cytochrome cd1 nitrite reductase, Electrochim. Acta. 48 (2003) 1055–1064, https://doi.org/10.1016/S0013-4686(02)00843-5.